

1 Marine submicron aerosol sources, sinks and 2 chemical fluxes

3
4 D. Ceburnis¹, M. Rinaldi², J. Keane-Brennan¹, J. Ovadnevaite¹, G.
5 Martucci¹, L. Giulianelli², C.D. O'Dowd¹

6 [1]School of Physics and Centre for Climate & Air Pollution Studies, Ryan
7 Institute, National University of Ireland, Galway, University Road, Galway,
8 Ireland

9 [2]Institute of Atmospheric Sciences and Climate, National Research Council,
10 Bologna, Italy

11 Correspondence to: D. Ceburnis (darius.ceburnis@nuigalway.ie)

12 13 Abstract

14 Aerosol physico-chemical fluxes over NE Atlantic waters were quantified
15 through the parallel deployment of micrometeorological eddy covariance flux
16 system and an aerosol chemistry gradient sampling system. Fluxes of primary
17 components, specifically, sea salt (SS), water insoluble organic carbon (WIOC)
18 and a combined sea spray are presented in the context of seasonality of marine
19 aerosol sources and sinks. The chemical gradients of secondary aerosol
20 components, specifically, nitrate, ammonium, oxalate, amines, methanesulfonic
21 acid (MSA) and water soluble organic nitrogen (WSON) were examined in great
22 detail. A strong power law relationship between fluxes and wind speed has been
23 obtained for primary sea salt and sea spray while water insoluble organic matter
24 (WIOM) followed a linear dependency. The power law relationship between sea
25 salt flux (F_{SS}) and 10m height wind speed (U_{10}) ($F_{SS}=0.0011U_{10}^{3.15}$) compared
26 very well with existing parameterisations but highlighted the divide between
27 parameterization derived from ambient observation versus laboratory
28 measurements. The observed seasonal pattern of sea salt production was mainly
29 driven by wind stress in addition to yet unquantified effect of marine OM
30 modifying fractional contributions of SS and OM in sea spray. WIOM wind
31 dependent fluxes were a complex combination of rising and waning biological
32 activity, especially in the flux footprint area, and wind-driven primary sea spray

33 production supporting the coupling of recently developed sea spray and marine
34 OM parameterisations.

35

36 **1. Introduction**

37 Marine aerosols contribute significantly to the global radiative budget and
38 consequently, changes in marine aerosol abundance and/or chemical composition
39 have an impact on climate change through both direct and indirect effects. The
40 Northeast Atlantic region is of particular interest due to a combination of
41 storminess, prevailing westerlies bringing marine air masses into continental
42 Europe, and biological activity in surface waters significantly affecting chemical
43 composition of atmospheric particulate matter (O'Dowd et al., 2004). Organic
44 matter (OM) has been observed in marine aerosol particles for many decades and
45 has been linked to fractional contribution of OM transferred from the sea-surface
46 into the tropospheric boundary layer through bubble-mediated production
47 processes (Blanchard, 1964; Hoffman and Duce, 1977; Middlebrook et al., 1998;
48 Oppo et al., 1999; Russell et al., 2010). There has been a significant progress in
49 understanding marine aerosol composition, which has been identified to consist
50 of significant amounts of organic matter (Cavalli et al., 2004; Sciare et al., 2009)
51 both water-soluble and water-insoluble. It has historically progressed from
52 mainly consisting of sea salt and non-sea salt sulphate (Charlson et al., 1987;
53 O'Dowd et al., 1997) to complex primary biogenic organic mixtures and states
54 (dissolved, particulate, colloidal or nanogel) (Cavalli et al., 2004; Leck and Bigg,
55 2005; Russell et al., 2010; Decesari et al., 2011) as well as secondary organic
56 compounds like organic acids (Kawamura and Sakaguchi, 1999; Mochida et al.,
57 2002; Turekian et al., 2003; Rinaldi et al., 2011) and recently discovered
58 biogenic amines (Facchini et al., 2008a; Muller et al., 2009). The findings of
59 Ceburnis et al. (2008) and Facchini et al. (2008b) independently confirmed that
60 water insoluble organic carbon (WIOC) in marine atmosphere has primary origin
61 while water soluble organic carbon (WSOC) is mainly secondary or processed
62 primary (Decesari et al., 2011), however, studies of Keene et al. (2007) and
63 Russell et al. (2010) evidenced that even WSOC can largely be of primary origin.
64 After significant fraction of marine sea spray particles was found to contain
65 biogenic organic matter compounds (O'Dowd et al., 2004) it became even more
66 important to determine principal sources and sinks of marine organic matter.

67 Tentatively, the source of biogenic marine organic matter has been linked to the
68 ocean surface and driven by a biological activity in surface waters based on a
69 seasonality pattern of organic matter and chlorophyll-a (Yoon et al., 2007; Sciare
70 et al., 2009) or regression analysis (O'Dowd et al., 2008; Russell et al., 2010).
71 Furthermore, the first quantitative estimate of submicron aerosol organic matter
72 in oceanic environment has been performed by Ceburnis et al. (2011) using dual
73 carbon isotope analysis that showed over 80% of organic matter in clean marine
74 air masses is of marine biogenic origin. A pilot study based on concentration
75 gradient method performed in marine environment by Ceburnis et al. (2008)
76 revealed that water soluble organic matter is largely produced by secondary
77 processes while water insoluble organic matter is of primary origin. The latter
78 study evaluated the first wind speed dependent fluxes, but those remained
79 uncertain due to the absence of parallel eddy covariance measurements and a
80 limited sampling period. Considering a significant seasonal cycle of marine
81 organic matter is important to study chemical fluxes on a full year basis to
82 capture the variability in aerosol sources and sinks.

83 This study is the extension of the study by Ceburnis et al. (2008) through the
84 combination of eddy covariance measurements in parallel with the off-line
85 chemical analysis of samples, expansion of the range of chemical species and
86 extension of the timescale to evaluate fluxes as a function of season.

87

88 **2. Experimental methods**

89 The flux of sea-spray aerosols has been studied previously as sea salt mass fluxes
90 or aerosol size and number flux (O'Dowd and De Leeuw, 2007; de Leeuw et al.,
91 2011). Apart from few studies, the flux experiments have typically focused on
92 super-micron sized particles. Eddy covariance method for studying submicron
93 particle fluxes was first used by Buzorius et al. (1998) estimating submicron
94 particle fluxes and sinks and has been since applied in a variety of environments:
95 boreal and tropical forest (Buzorius et al., 1998; Ahlm et al., 2009), ocean
96 (Nilsson et al., 2001; Geever et al., 2005; Norris et al., 2008; Brooks et al., 2009),
97 desert (Fratini et al., 2007) and urban (Martensson et al., 2006; Martin et al.,
98 2009). Eddy-covariance method is typically used to study total particles fluxes.
99 The technique has been modified into relaxed eddy-covariance method to allow
100 studying size-segregated particle fluxes (Gaman et al., 2004) or disjunct eddy

101 covariance method (Held et al., 2007) employing slower response instruments. It
102 should be noted, however, that while number of sea spray particles is dominated
103 by submicron particles, mass is dominated by super-micron sizes and not a single
104 method is capable of measuring particles around the important boundary of 1
105 micrometer. None of the above techniques were suitable for studying chemically
106 resolved fluxes, because chemical analysis typically requires long sampling time
107 (many hours for off-line chemical analysis). Most recently, however, eddy-
108 covariance system coupled with high resolution aerosol mass spectrometer has
109 been used to study chemically resolved fluxes (Nemitz et al., 2008; Farmer et al.,
110 2011), but those were largely limited to areas with relatively high concentration
111 of species.

112 The study of chemical fluxes in a relatively clean marine atmosphere represents a
113 great challenge due to generally low absolute species concentrations and the lack
114 of appropriate experimental methods. The rationale of choosing the gradient-flux
115 method was based on the fact that persistent fluxes must produce concentration
116 gradients with their sign depending on the source and assuming that recurrent
117 eddies allow sampling for certain number of hours to meet analytical
118 requirements of chemical species. Additional challenges exist when it comes to
119 reactive species (organic matter) due to chemical transformation during transport
120 to the sampling location or extended sampling durations. A combination of
121 continuous production (or removal) of particles and turbulent eddies of varying
122 magnitude within the boundary layer should establish concentration profiles. The
123 profiles, therefore, are a net result of the competition between upward and
124 downward eddies averaged over time. The persistent surface source will manifest
125 itself in a decreasing concentration away from the source. The absence of the
126 surface source should result in an increasing concentration profile as particles are
127 removed to the surface through deposition processes. For the approach to work
128 one needs neutral or near-neutral boundary layer stability conditions persisting
129 for sufficient timescales to allow sampling over many hours. The biggest caveat
130 is whether representative averaging over many hours can produce meaningful
131 results. The approach was previously demonstrated to work in urban
132 environment (Valiulis et al., 2002) as well as in a relatively clean marine
133 environment (Ceburnis et al., 2008). This study is the continuation of the latter

134 study adding full scale eddy-covariance system and expanding the number of
135 chemical species studied.

136 A new set-up to study gradient chemical fluxes was installed at Mace Head
137 Atmospheric Research Station on the west coast of Ireland (Jennings et al., 2003;
138 O'Connor et al., 2008) comprising PM1 samplers installed at three different
139 heights (3 m, 10 m, and 30 m) while the eddy covariance system installed at the
140 22 meter height.

141 LIDAR measurements (Jenoptik/Lufft and Vaisala ceilometers) are continuously
142 conducted at Mace Head and a dedicated algorithm for temporal height tracking
143 (THT) (Haefelin et al., 2012; Milroy et al., 2012) using the backscatter profiles
144 measured by the LIDAR was used to identify the surface mixed layers (SML)
145 and the decoupled residual layers (DRL), both important parameters when
146 considering boundary layer filled by primary fluxes.

147 The chlorophyll satellite data (daily, 1° spatial resolution) were obtained from
148 GlobColour (<http://www.globcolour.info>). They result from the merging of
149 Medium-Resolution Imaging Spectrometer (MERIS), Moderate Resolution
150 Imaging Spectroradiometer (MODIS), and Sea-viewing Wide Field-of-view
151 Sensor (SeaWiFS) data, using advanced retrieval based on fitting an in-water
152 biooptical model to the merged set of observed normalized water-leaving
153 radiances. A thorough description of the data treatment can be found in Rinaldi et
154 al.(2013).

155

156 **2.1 Sampling strategy**

157 Meteorological records demonstrate that on average marine westerly air masses
158 account for over 50% of time at the station (Cooke et al., 1997; Jennings et al.,
159 2003). The gradient measurement system PM1 samplers (Sven Leckel
160 Ingenieurbüro GmbH) ran in parallel at a flow rate of 38 lpm. Samples were
161 collected in clean marine conditions (wind direction $190 < WD < 300$ and
162 Condensation Particle Counter (CPC) concentrations $< 700 \text{ particles cm}^{-3}$) using
163 an automated sampling system on quartz filters for the analysis of both organic
164 and inorganic components of marine aerosol. The system operated day and night
165 whenever the above clean marine conditions were met. Active control of the
166 sampling conditions excluded sampling during occasional short-term spikes of
167 CPC concentrations either due to coastal nucleation events or occasional local

168 ship traffic. Post-sampling analysis revealed that such air masses did not have
169 contact with land for 4-5 days (as confirmed by air mass back-trajectories) and
170 black carbon (BC) concentration measured by an Aethalometer (AE-16, Magee
171 Scientific, single wavelength at 880 nm) did not exceed 50 ng m^{-3} . Such air
172 masses have been typically spending the last 48 hours (at least) in the marine
173 boundary layer as documented by Cavalli et al. (2004) and Ceburnis et al. (2011).
174 The latter study quantitatively demonstrated that in clean marine air masses
175 anthropogenic carbon species typically contributed to 8-20% of the total carbon
176 mass which should be applicable to other anthropogenic species due to internally
177 mixed anthropogenic aerosol far from the source. It is important to note that
178 clean marine samples collected at Mace Head are representative of the open
179 ocean environment considering chemical and physical similarities between open
180 ocean and coastal (Mace Head) samples (Rinaldi et al., 2009). The marine air
181 criteria used at Mace Head were demonstrated to be sufficient at ensuring that
182 anthropogenic and coastal effects are minimised to guarantee a dominant, if not
183 at times overwhelming natural marine aerosol signal as detailed in the study of
184 O'Dowd et al.(2014).

185

186 **2.2 Off-line chemical analysis and concentration gradients**

187 Fifteen PM1 gradient samples were collected during 13 month period in clean
188 marine conditions as listed in Table 1. The sampling strategy aimed at capturing
189 two samples per month providing that clean marine conditions were prevailing
190 and each sample duration lasted on average 50% of time during the calendar
191 week.

192 The samples were analysed for a wide range of chemical species present in
193 aerosol particles: sodium (a marker for sea salt (SS)), non-sea-salt sulphate
194 (nssSO_4), nitrate (NO_3), ammonium (NH_4), methanesulphonic acid (MSA), total
195 carbon (TC), oxalate (Oxa), (analytical details can be found in Cavalli et al.
196 (2004)), water soluble organic carbon (WSOC), water insoluble organic carbon
197 (WIOC) (Rinaldi et al., 2009), water soluble organic nitrogen (WSON), total
198 nitrogen (TN), dimethylamine (DMA) and diethylamine (DEA) (Facchini et al.,
199 2008a). WIOC was calculated as $\text{WIOC}=\text{TC}-\text{WSOC}$ while WSON was
200 calculated as $\text{WSON}=\text{TN}-\text{WSIN}$ (water soluble inorganic nitrogen). WSOM
201 (water soluble organic matter) was calculated as $\text{WSOC}*1.8$ and WIOM (water

202 insoluble organic matter) was calculated as $WIOC \times 1.4$ (Decesari et al., 2007;
203 Facchini et al., 2008b). Sea salt concentration was calculated as $SS = Na \times 3.1$
204 (Seinfeld and Pandis, 2006). The absolute concentration ranges of all measured
205 components are summarised in Table 2.

206 Normalised averaged concentration profiles of all measured chemical species
207 were obtained as follows: for each aerosol component, only samples for which
208 concentrations above the detection limit were observed at all three sampling
209 altitudes were used in data analysis. Normalisation was done by dividing the
210 concentration at every height by the sum concentration of three levels thus giving
211 the same weight to every profile for averaging purposes. After normalisation, the
212 profiles of each mass category were averaged, resulting in statistically
213 meaningful variances around the mean value and presented as an average and its
214 standard deviation. The normalised averaged concentration profiles allowed
215 classification and categorisation of the profiles, but the normalised data were not
216 used for calculating gradients and fluxes. The main features were similar to the
217 ones documented by (Ceburnis et al., 2008): decreasing concentration with
218 height, or negative gradient, was common of species produced at the surface by
219 primary processes while increasing concentration with height, or positive
220 gradient, was common of species produced by secondary processes in the
221 atmosphere aloft or within the marine boundary layer.

222 Concentration gradients of various chemical species were obtained by linear fit
223 of the concentration profile (except WSOM). A detailed discussion of potential
224 influence of local sources (surf-zone) to the gradient can be found in (Ceburnis et
225 al., 2008) and reconsidered in the Results section.

226

227 **2.3 Eddy-covariance system**

228 Eddy-covariance measurements of micrometeorological parameters, water
229 vapour (H_2O) and CO_2 fluxes were undertaken in parallel (Keane-Brennan,
230 2011) which provided micrometeorological measurement data for calculating
231 gradient fluxes. The flux package comprised a Solent sonic anemometer (Gill
232 Windmaster Pro) to provide 3-D wind fields at 10 Hz. The sonic anemometer
233 was mounted 2 meters out from the sea-facing side of the 22 m tower and a
234 turbulent flow around the tower (Buzorius et al., 1998). Flux data were averaged
235 for 30 min for further analysis and more details on flux data can be found in

236 Geever et al. (2005) and Keane-Brennan et al. (2011). Half-hourly flux data were
237 further averaged to match the periods of gradient samples. The undertaken
238 strategies allowed a complete analysis of the source and sink fluxes as a function
239 of wind speed and oceanic biological activity and provided a quantification of
240 both primary and secondary inorganic and organic aerosol species cycling in the
241 marine boundary layer.

242

243 **2.4 Flux-gradient method**

244 First-order closure turbulent flux parameterisation, often known as a gradient
245 transport theory, K -theory or flux-gradient similarity method, can be expressed
246 according to Stull (1988) as following:

247

$$248 \quad F = -K_z \left. \frac{dc}{dz} \right|_z \quad (1)$$

249 where F is the flux, K_z is the turbulent-transfer coefficient; dc/dz is the
250 concentration gradient.

251

252 Thus having K_z value and the measured concentration gradient it is possible to
253 calculate fluxes of chemical species. The approach, however, would only allow
254 calculating the net flux and does not allow distinguishing between upward and
255 downward fluxes in high time resolution as is typically done with the eddy
256 covariance system. The K_z parameter can be calculated from the eddy covariance
257 (EC) measurements using high frequency data of vertical wind velocity using the
258 formula: $\sigma = \sqrt{2K_z/t}$ (where σ is the standard deviation of vertical wind velocity,
259 K_z is the turbulent-transfer coefficient, and time is the unit time (1s)) which
260 follows from diffusivity fundamentals (e.g. (Reible, 1998)) applied to the vertical
261 wind speed. K_z had to be averaged over about 50 to 140 hours to represent the
262 sampling period of a particular concentration profile. The averaged K_z values
263 were compared with eddy covariance data and presented in Figure 1 to check
264 whether the averaged K_z values were consistent with the high time resolution
265 measurements. The dependence of K_z values on horizontal wind speed were very
266 similar pointing to the fact that K_z values were consistently distributed around the
267 mean and the mean average representing gradient samples was statistically
268 meaningful. The variance of K_z values around the mean provided the partial

269 uncertainty in flux calculations. It is worth noting that the power law coefficient
270 of the averaged K_z (WS) dependence was very similar to the one given by
271 Ceburnis et al. (2008) (1.97 and 2.07 respectively). A similarity between the
272 relationships obtained by Ceburnis et al. (2008) from 2002 EC data and this
273 study period (2008-2009) suggests that the dynamics of the boundary layer did
274 not change significantly over time at this geographical location, thereby
275 providing a confidence that the K_z values can be reliably derived from the
276 horizontal wind speed measurements if the K_z values cannot be estimated
277 directly. A tight relationship between K_z and horizontal wind speed and the
278 absence of a diurnal cycle of K_z is typical in wind shear generated turbulence
279 environment like marine sector at Mace Head. Consequently, the above
280 relationship between horizontal wind speed and the coefficient of turbulent
281 transfer would only apply to the marine sector and Mace Head location. The
282 scatter of K_z values over a short or long period of time was mainly due to
283 gustiness as presented in Figure 2 where the K_z and wind speed relationship was
284 coloured by normalised standard deviation of the horizontal wind using random
285 subset of data. All elevated values of K_z were accompanied by high values of the
286 standard deviation of the horizontal wind speed. Therefore, K_z values were all
287 meaningful and must have been included in the mean average to represent fast
288 turbulent eddies.

289 It is important to know the thickness of the surface layer as it is here that fluxes
290 are considered to be constant and gradients adhere to similarity theory. Another
291 caveat is the formation of internal boundary layers (Stull, 1988). Detailed
292 measurements performed during NAMBLEX campaign at Mace Head (Heard et
293 al., 2006) provided strong evidence that the internal boundary layer had little
294 impact on the measurements made on the main tower if they were conducted
295 above 7-10 m (Coe et al., 2006; Norton et al., 2006), which would include two
296 out of our three sampling points. Norton et al. (2006) showed that the internal
297 boundary layer was typically limited to below 10m and never propagated to the
298 top of the tower in marine sector, consequently, having small effect on our
299 measurements at 10 m and 30m. Coe et al. (2006) concluded that over a wide
300 range of aerosol sizes there was no impact of the inter-tidal zone or the surf zone
301 on measurements made at 7 m above ground level or higher.

302

303 2.5 Errors and uncertainties

304 The flux-gradient method based on the Equation 1, involves several variables,
305 necessitating a calculation of the combined propagated uncertainty. Specifically,
306 not only it involved two independently measured concentrations at two heights,
307 but the uncertainty of the subtracted blank concentration (pre-fired but not
308 exposed filter) and the uncertainty of the K_z value. The combined fractional
309 uncertainty of an individual flux was calculated by the following Equation:

310

$$311 \quad \delta q = \sqrt{\left(\frac{\partial q}{\partial x_1} \delta x_1\right)^2 + \dots + \left(\frac{\partial q}{\partial x_n} \delta x_n\right)^2} \quad (2)$$

312 where x_i are the independent variables and δx_i are the fractional uncertainties of
313 the independent variables.

314 The uncertainty of individual concentrations (C) (provided in Table S1) and the
315 gradient (G) was calculated by the following Equations:

$$316 \quad \delta C = \sqrt{(\delta C_{meas})^2 + (\delta C_{blank})^2} \quad (3)$$

$$317 \quad \delta G = \sqrt{(\delta C_{10})^2 + (\delta C_{30})^2} \quad (4)$$

318 where C_{meas} , C_{blank} , C_{10} and C_{30} were measured, blank and concentration at 10
319 and 30 meters, respectively.

320 The relative uncertainty of the corresponding fluxes was calculated by the
321 following Equation based on multiplication of measured quantities ($F=G*K_z$):

$$322 \quad \frac{\delta F}{F} = \sqrt{\left(\frac{\delta G}{G}\right)^2 + \left(\frac{\delta K_z}{K_z}\right)^2} \quad (5)$$

323 where G and K_z are corresponding gradients and coefficient of turbulent transfer,
324 respectively. Note that the flux uncertainty is dominated by the gradient
325 uncertainty, because the uncertainty of turbulent transfer coefficient would be
326 actually smaller than presented in Eq. 5 due to being an average of over a
327 hundred of half-hourly values.

328 The relative uncertainty of the organic matter fractional contribution to sea spray
329 ($OM_{ss}=WIOM/(WIOM+SS)$), where the variable $WIOM$ appeared in both
330 nominator and denominator and $WIOM$ represented total sea spray OM, resulted
331 in a more complicated equation of the combined propagated uncertainty of the
332 OM fractional contribution:

$$333 \quad \frac{\delta OM_{ss}}{OM_{ss}} = \frac{SS}{(SS+WIOM)} \sqrt{\left(\frac{\partial WIOM}{WIOM}\right)^2 + \left(\frac{\partial SS}{SS}\right)^2} \quad (6)$$

334 where the ratio in front of the square root is the fractional contribution of sea salt
335 in sea spray resulting in the fractional uncertainty of the OM fractional
336 contribution dependent on the sea salt fractional contribution and, therefore,
337 always smaller than the additively combined fractional uncertainty of sea salt and
338 WIOM measurement.

339 The uncertainty of the fitted functional relationships obtained from the discretely
340 measured values was presented with the 95% confidence bands which was
341 conceptually different from the fractional uncertainties of individual values. The
342 confidence bands also helped to define the best fitted function (e.g. linear or
343 power law) as unrealistic fits had very low or no confidence at all. Typically, the
344 confidence bands become narrower as the number of points increases and/or their
345 scatter decreases. The presentation of the confidence bands provided the physical
346 meaning of the points residing outside the confidence bands. An individual point
347 which is outside the confidence bands suggests a higher order of the relationship
348 or an unaccounted freak error. Several of such cases will be discussed
349 accordingly.

350

351 **3 Results and Discussions**

352 The measurements at three different heights allow resolving the vertical
353 concentration profiles of different chemical species and the magnitude of the
354 sources and sinks, or corresponding fluxes, shape the profiles. Most of them were
355 non-linear, but well interpretable having studied concentration and flux footprints
356 in detail in the previous pilot study of (Ceburnis et al., 2008). It is important to
357 note that the footprint of the measured absolute concentration was of many tens
358 to hundreds of kilometres offshore while the footprint of the concentration
359 gradient or the flux was within about 10km from the measurement location, i.e.
360 coastal waters (Ceburnis et al., 2008). The surf zone emissions may have had
361 certain influence on the concentrations of sea salt or sea-spray at the lowest level
362 of 3m, particularly for low wind speeds, practically disappearing at higher
363 winds(O'Dowd et al., 2014), but had little or no impact on secondary organic
364 aerosol. The different distances of the flux footprint arise from emissions
365 contributing to the concentration at different heights. The flux footprint of the
366 90% concentration difference between 3 and 10 meters is 0.2-1.2 km while the
367 footprint of the 90% of the difference between 10 and 30 meters extends to 5 km

368 (Figure 1, Ceburnis et al. 2008). The remaining 10% of the contribution extends
369 well beyond 5km, perhaps 10 km distance being a safe approximation. A
370 condensation potential could have also contributed to the concentration
371 differences of certain species as the time required for the air parcel to cover 10
372 km distance is about 15 min which is more than sufficient to achieve gas-aerosol
373 equilibrium, e.g. (Meng and Seinfeld, 1996; O'Dowd et al., 2000).

374

375 **3.1 Concentration gradient profiles**

376

377 **3.1.1 Primary components**

378 The concentration profile of sea salt (top left in Figure 3) was unambiguously
379 surface sourced or primary, i.e. concentration was decreasing vertically. Some of
380 the individual profiles were sharper than others, but all were primary with only
381 three exceptions where the profiles were distorted at lower heights possibly
382 partly due to measurement errors and partly due to boundary layer dynamics and
383 changes in sea state during the sampling period (ascending and descending wind
384 regimes). However, as it was stated above, surf-zone emissions could have had
385 influenced the concentration value at the lowest level of 3 meters and, therefore,
386 this level was not used in the flux calculations of primary sea spray species.

387 Interestingly, similar “negative gradient” concentration profiles were obtained
388 for nitrate and oxalate. **However, those profiles were slightly, but repeatedly**
389 **(systematically) distorted,** i.e. the concentrations of oxalate and nitrate
390 significantly diverged from the sea salt one at the lowest sampling height of 3
391 meters while following the sea salt profile above 10 meters. It is well established
392 that nitrate is produced by secondary processes and mainly manifesting itself
393 through condensed nitric acid on pre-existing sea salt particles in the absence of
394 anthropogenic ammonium nitrate. Sea salt particles at the lowest level were the
395 freshest having the closest flux footprint and, consequently, adsorbed the least
396 amount of condensable nitric or oxalic acid compared to higher levels. Similarly
397 to nitrate, oxalic acid could have been condensing on pre-existing sea salt
398 particles as well despite more diverse chemical pathways of oxalic acid (some of
399 the oxalate could also be produced by oxidation of organic matter inside sea-
400 spray particles (Rinaldi et al., 2011) and, therefore, manifesting itself as
401 “primary” species. The concentration profile of oxalic acid was similar to that of

402 nitrate and could indicate that a significant amount of oxalate is produced in the
403 atmosphere aloft subsequently condensing onto primary sea spray particles due
404 to its acidic nature.

405 The water insoluble organic matter (WIOM) concentration profiles were split
406 between three main categories: production (5 profiles), removal (6 profiles) and
407 mixed profiles (4 profiles) (bottom right of Figure 3). Given that fractional
408 contribution of OM in primary sea spray is related to the enrichment of organic
409 matter at the ocean surface, this range of behaviour can be interpreted in terms of
410 the location of biologically active region relative to the flux footprint. The wind
411 speed has been reported to have an effect on fractional contribution of OM, but
412 quantitative effect is unclear and will be discussed in more detail in chapter 3.4.
413 The biologically active water patches within the flux footprint (~10 km from the
414 measurement location) were responsible whether WIOM was produced or
415 removed from the surface layer, or a combination of both processes. Therefore, a
416 mixed profile was pointing at the production at a longer distance from the coast
417 and the removal close to the measurement location. Thus the removal profile was
418 pointing both at the deposition within the flux footprint area and/or the absence
419 of biological activity in surface waters within the flux footprint area. The WIOM
420 production by the secondary processes cannot be completely excluded either, but
421 we have no evidence of that. It is worth noting that the production profiles were
422 observed in early spring (March until early May) when biological activity is high
423 at the coast and during late summer (late July-August) when biological activity
424 has a second maximum identified by the chlorophyll proxy (Yoon et al., 2007).
425 In contrast, the removal profile was observed during late spring and early
426 summer when biological activity is retreating away from the coast into the open
427 ocean. Despite a general pattern of the evolution of biological activity presented
428 by Yoon et al. (2007) it should be stressed that biological activity is very patchy
429 all over the ocean including coastal areas and the phytoplankton blooms are
430 generally governed by the availability of nutrients which themselves are supplied
431 by ocean currents and upwelling and become unpredictable on a day-to-week
432 time scale.

433

434 **3.1.2 Secondary components**

435 The inorganic secondary species (nssSO_4 and NH_4) are presented in top right of
436 Figure 3 along with an aerosol neutralisation profile considering only ammonium
437 and sulphate which will be discussed later. Ammonium profile was clearly
438 secondary, as expected, due to ammonia being the principal gaseous neutralizing
439 agent in the marine boundary layer. It should be noted that the concentration
440 profile of nssSO_4 was pretty constant and did not follow that of the ammonium
441 profile as it could be expected considering that sulphuric acid is the main acidic
442 species in the marine boundary layer, typically neutralized by ammonium.
443 NssSO_4 was calculated as the difference between two relatively large numbers
444 (total measured SO_4 minus sea-salt SO_4 as inferred from a conservative tracer
445 such as Na ion). As sea salt concentration was changing quite dramatically with
446 height especially in moderate to high wind speed during winter, some ambiguity
447 must be acknowledged before interpreting nssSO_4 profile. In fact, if the winter
448 sulphate profiles were excluded from the average that would have improved the
449 average profile. In any event nssSO_4 concentrations at three different heights
450 were not significantly different preventing any conclusions with respect to
451 apparently secondary nssSO_4 . The uncertainty in nss -sulphate determination can
452 be the reason of the difference with respect to the profile of ammonium. Looking
453 at the profiles, it can be observed that marine aerosol sampled at Mace Head is
454 more neutralized at 30 m than closer to the sea level (Figure 3 (top right) and
455 Figure 4), even though neutralization with respect to sulphuric acid is never
456 complete, due to scarcity of ammonia in the marine boundary layer. **Figure 4**
457 **shows calculated ammonium (considering neutralisation by sulphate only as**
458 **nitrate was more likely to be neutralised by sodium (causing chloride depletion)**
459 **due to scarcity of ammonia in the marine boundary layer) versus measured**
460 **ammonium revealing significant but consistent differences in neutralisation**
461 **pattern at three different heights.** The neutralization profile can be driven by the
462 gaseous ammonia vertical profile, which we have no hint about, or can be an
463 indication of the importance of in-cloud processes of sulphate neutralization
464 considering also that measurements at the lowest level were somewhat perturbed
465 due to surf-zone fluxes. In fact, if the neutralization of acidic sulphates occurred
466 prevalently in clouds, after scavenging of gaseous ammonia into acidic droplets,
467 this process would occur more likely at the top of the marine boundary layer,
468 were cloud layers form, justifying the observed neutralization profile.

469 The secondary organic species (MSA, WSOM and WSON) are presented in the
470 bottom left of Figure 3. The MSA exhibited a “mixed profile” with steep increase
471 of concentration between 3 and 10 m, typical of secondary products and
472 decreasing profile between 10 and 30 m, likely due to condensation of MSA on
473 sea salt particles (Hopkins et al., 2008) that causes an apparently primary profile.
474 A clear secondary profile was observed for WSOM also, reaffirming the
475 conclusion of Ceburnis et al. (2008) on the secondary origin of WSOM. The
476 water soluble organic nitrogen concentration pattern is presented in the bottom
477 left of Figure 3. WSON presents a mixed profile, therefore, it is not possible to
478 attribute it to primary or secondary formation processes unambiguously. WSON
479 concentration in aerosol samples is generally difficult to quantify as it is
480 calculated as the difference between the total nitrogen (TN) and the water soluble
481 inorganic nitrogen (WSIN) – both numbers of similar magnitude. As a result,
482 only 7 complete profiles could be derived out of 15 samples and should,
483 therefore, be considered cautiously (8 profiles were discarded as incomplete, i.e.
484 missing determined concentration at one or two levels). Along with WSON,
485 aliphatic amines were analysed following Facchini et al. (2008a). WSON, DMA
486 and DEA are minor constituents of marine aerosol, together typically accounting
487 for 10% of secondary organic aerosol (Facchini et al., 2008a). While the
488 magnitude of their absolute concentrations may be misleading – amines can be
489 important species facilitating new particle production in the marine atmosphere
490 (Dall’Osto et al., 2012) – quantification of their concentration by offline chemical
491 analysis is always challenging. Mostly concentrations of DMA and DEA at the
492 lowest height were below detection limit and, therefore, no profile can be
493 provided for these species with confidence. However, the fact that detectable
494 concentrations were always observed at 30 m, strongly suggests a secondary
495 origin for DMA and DEA.

496 The well-established aerosol chemical compounds such as nitrate, oxalate, MSA
497 and less well established WSON were all studied for the first time using flux-
498 gradient method. The concentration profiles of the above compounds have not
499 demonstrated that the species were secondary, despite well-established
500 knowledge of their secondary formation in the atmosphere aloft (boundary layer,
501 clouds or free troposphere)(Seinfeld and Pandis, 2006; Facchini et al., 2008a;
502 Rinaldi et al., 2011). Figure 5 is presented for elucidating an apparent “primary”

503 profile of nitrate and oxalate which is due to aforementioned species condensing
504 or reacting with sea spray particles. MSA by contrast has the weakest if any
505 relationship with sea salt. Figure 5 (top left) presents the relationship between
506 nitrate and sea salt mass which appears as linear with the exception of 2-3
507 outliers. The outliers likely appeared due to the presence of trace amounts of
508 ammonium nitrate. Ammonium nitrate is generally considered as anthropogenic
509 species and can be present in trace amounts due to pollution background. The
510 trace amount was really small, 20-30 ng m⁻³ of nitrate only re-affirming
511 cleanness of the marine atmosphere studied at Mace Head. Despite a strong
512 similarity in concentration pattern of nitrate and primary sea salt it is
513 inconceivable that a significant amount of primary nitrate can be produced
514 (nitrate is a tracer nutrient in sea water) and, therefore, must be derived by
515 condensation of nitric acid on pre-existing sea salt.

516 The relationship of sea salt and oxalate (top right plot of Figure 5) was slightly
517 different from nitrate and somewhat similar to MSA. While oxalate can indeed
518 condense on pre-existing sea salt particles its chemical pathways of secondary
519 production are different and more diverse than that of nitrate as were detailed by
520 Rinaldi et al. (2011). Oxalate can also be present in sea-spray particles via
521 oxidation of organic matter in sea-spray and, therefore, dependent on biological
522 activity of the ocean. As opposed to nitrate, the oxalate was not enhanced in the
523 presence of copious amounts of sea salt particles suggesting that oxalic acid is
524 not an ever present species in the boundary layer which would readily condense
525 on sea salt. The same was true for MSA which showed even less of a relationship
526 with the sea salt mass (bottom left of Figure 5). MSA production is
527 photochemically driven and time limited considering the gradient footprint of
528 0.2-10 km in the coastal zone. The water soluble organic nitrogen (WSON) is a
529 relatively less studied class of chemical compounds of which amines are the best
530 known compounds (Facchini et al., 2008a). The observed concentrations of
531 DEA, DMA and WSON were very similar to the ones documented by Facchini et
532 al. (2008a) in clean marine air masses. Both WSON and the sum of
533 dimethylamine (DMA) and diethylamine (DEA) exhibited a relationship with
534 water soluble organic carbon (WSOC) (bottom right of Figure 5), however, only
535 WSOC and WSON correlated at a significant level ($r = 0.58$). Note, that the sum
536 of amines is presented in absolute concentration while that of WSON as a mass

537 of nitrogen. The comparison between the WSON and the sum of amines
538 suggested that the amines were likely the dominant species of WSON, but
539 difficult to determine due to detection limit as noted above.
540 WSOC/WSON/DEA/DMA relationship is presented in Figure 5 (bottom right)
541 for exploratory purposes as these interrelationships have not been examined or
542 discussed in the context of marine aerosol.

543

544 **3.2 Chemical fluxes**

545

546 **3.2.1 Sea salt flux**

547 The individual concentration profiles had to be fitted first in order to calculate
548 gradients and then fluxes using Equation 1. The concentration gradient is a
549 derivative of the concentration as a function of height. The lowest level at which
550 concentration was measured was at 3 meters and may have been affected by surf-
551 zone fluxes as discussed in detail by Ceburnis et al. (2008). Therefore, only the
552 concentrations measured at 10 and 30m were used in calculating primary fluxes
553 in order to reduce surf-zone related uncertainty in calculated fluxes. This
554 approach yielded “linear gradients” and constant fluxes. It is important to note
555 that for comparison purposes K_z values were adjusted for 10m wind speed from
556 Figure 1 given well established relationship between K_z values and the horizontal
557 wind speed as well as good agreement between EC and gradient samples. Sea
558 salt (SS) and sea-spray (SS+WIOM) flux dependence on the wind speed is
559 presented in Figure 6. The uncertainty parameters of all the fitted flux-wind
560 speed relationships are summarised in Table 3. The obtained relationship was the
561 power law very similar to the one obtained by Ceburnis et al. (2008), but this
562 time it was quantified separately for sea salt and sea-spray. The relationship of
563 sea-spray flux was stronger; however, inherent uncertainty had to be considered.
564 The K_z values were calculated explicitly and, therefore, the uncertainty of the
565 flux was down to the uncertainty of the gradient which in turn was dependent on
566 the accuracy of the chemical analysis. The uncertainty of the individual sea salt
567 fluxes was calculated as a combined propagated uncertainty of the two
568 concentrations (10 and 30m height) and the uncertainty of K_z values. The
569 uncertainty of the fitted relationship was presented as the 95% confidence bands.
570 Typically, the confidence bands would narrow constraining the relationship as

571 the number of points increase and/or their scatter decreases. The power law
572 exponent of SS and sea spray (3.15 & 3.4) source function were very similar to
573 SS source function obtained by Ovadnevaite et al. (2012) who obtained power
574 law exponent of 2.7 using high resolution measurements with aerosol mass
575 spectrometer. The maximum sea salt flux calculated by flux-gradient method was
576 $2\text{-}3 \text{ ng m}^{-2} \text{ s}^{-1}$ at the maximum average wind speed of $11\text{-}12 \text{ m s}^{-1}$ while the mass
577 flux range presented by Ovadnevaite et al. (2012) was $15\text{-}20 \text{ ng m}^{-2} \text{ s}^{-1}$ at 25 m s^{-1}
578 hardly in need of extrapolation to even higher wind speed. However,
579 quantitatively both studies (this study and Ovadnevaite et al. (2012)) agreed well
580 for a given wind speed of e.g. 10 m s^{-1} , 1.67 and $1.97 \text{ ng m}^{-2} \text{ s}^{-1}$, respectively.
581 Only two of the individual fluxes lay outside the 95% confidence bands
582 suggesting that the linear flux-gradient method is not the ideal one - it is an
583 approximation after all. It is suspected that the necessitated long averaging time
584 of the sample was an important reason behind it as well.

585

586 **3.2.1 Organic matter flux**

587 The corresponding chemical flux of WIOM was calculated and presented in
588 Figure 7 (left). All uncertainty considerations are the same for the sea salt and
589 sea-spray fluxes. There was one important difference, however; the WIOM
590 fluxes turned out to be positive only at relatively strong wind speed exceeding 7
591 m s^{-1} while all WIOM fluxes below this value were negative (with consequential
592 large intercept), pointing at the removal or deposition of WIOM. Note, that the
593 negative fluxes corresponding to lower wind speed were obtained from removal
594 profiles introduced previously in chapter 3.1.1. That does not mean that the
595 production flux becomes negative at low wind speed, but rather reflects
596 observations when the production flux at very low wind speed in the gradient
597 footprint area is smaller than the deposition flux of WIOM generated tens to
598 hundreds kilometres away. Therefore, the resulting negative WIOM flux at low
599 wind speed occurred due to the absence of biological activity in the flux footprint
600 area (within $\sim 10 \text{ km}$ from the measurement location). Another possibility is that
601 there is no measurable concentration increase in WIOM mass at wind speeds
602 below 7 m s^{-1} resulting in the negative flux as WIOM is being removed from the
603 surface layer due to the largely absent source.

604 The WIOM flux was best fitted to the linear function (all other functional forms
605 were associated with uncertainties far larger than the coefficient values) and
606 there were reasons why it might be so. The WIOM content in sea spray depends
607 on two processes: (1) fractional contribution of OM to sea spray as a function of
608 biological activity and/or organic matter concentration and physico-chemical
609 state in sea water; and (2) sea spray production flux as a function of wind stress
610 or wave state. The two processes are independent and combine differently during
611 different seasons. For example, during summer the fractional contribution of OM
612 is typically higher, but the sea spray flux is typically lower while during winter
613 the production flux would typically be high (due to deeper low pressure systems
614 generating higher wind speeds), but the fractional contribution of OM would be
615 the lowest.

616 The water soluble organic matter exhibited the removal gradient throughout the
617 study period which allowed studying a seasonal pattern of a sink and a
618 dependence on meteorological parameters. Individual WSOM concentration
619 profiles were first fitted to power law using concentrations at all three heights
620 and then the resulting fluxes were calculated by the Equation 1 at 10 meter
621 height. The reason why all three heights were used is that WSOM concentration
622 profiles pointed to a well-established removal profile with the surf-zone having
623 minimal if any impact. The removal rate dependence on the wind speed is
624 presented in Figure 7 (right) and attempted to fit to the power law. It turned out
625 that the WSOM removal rate or sink was dependent on the wind speed, but with
626 the large uncertainty and, therefore, declared unreliable. Due to the large
627 uncertainty of the individual fluxes the actual removal rate was uncertain too, but
628 worth noting that the removal rate of WSOM was opposite in sign to WIOM
629 production flux.

630

631 **3.3 A comparison with the other flux-wind speed relationships**

632 Given the uncertainty of the derived sea salt flux and wind speed
633 parameterisation it was important to compare it with other available source
634 functions. Equally important was to cover a wide range of methods used to
635 derive fluxes. Figure 8 presents the source functions for which submicron sea salt
636 mass could have been calculated and include the following: Callaghan (2013),
637 Clarke et al. (2006), Fuentes et al. (2010), Gong-Monahan (Gong, 2003),

638 Martensson et al. (2003), Ovadnevaite et al. (2012; 2013) and this study. Clarke
639 et al. (2006), Fuentes et al. (2010) and Martensson et al. (2003) parameterisations
640 were derived in either laboratory conditions or in-situ surf breaking waves and
641 coupled with Monahan and Muircheartaigh (1980) whitecap parameterisation to
642 yield flux wind speed relationship. All of the above parameterisations were based
643 on exploring SMPS measurement data. Gong et al. (2003) used an original
644 Monahan (Monahan et al., 1982) parameterisation obtained in the laboratory
645 experiment and adjusted for the size range $<0.2 \mu\text{m}$. Callaghan (2013) used in-
646 situ whitecap measurements developing a discrete whitecap method and Gong
647 (2003) parameterisation to obtain submicrometer sea salt mass flux and wind
648 speed parameterisation. While the Callaghan (2013) paper proposes a new SSA
649 source function, it pulls the whitecap parameterisation from the Callaghan et al.
650 (2008) paper. One of the primary findings of the Callaghan (2013) work was the
651 importance of choosing the correct whitecap timescale for the discrete whitecap
652 method in particular. Finally, Ovadnevaite et al. (2012; 2013) and flux-gradient
653 method of this study used ambient measurement data (real-time AMS sea salt
654 measurements, SMPS measurements and PM1 gradient measurements,
655 respectively), but were completely independent of each other and different in
656 terms of the utilised methods. It should be noted, that despite the fact that the
657 latter methods estimated net fluxes as opposed to production fluxes measured in
658 the laboratory experiments, deposition fluxes are typically small, in the order of
659 2-4% in submicron particle range (Hoppel et al., 2002). The presented
660 parameterisations fall into two regimes as seen in Figure 9: Clarke et al. (2006),
661 Fuentes et al. (2010), Gong (2003) and Martensson et al. (2003)
662 parameterisations exhibit a significantly higher wind-speed dependency
663 compared to the more recent parameterisations by Callaghan (2013),
664 Ovadnevaite et al. (2012; 2013) and this study. Note, that all the latter
665 parameterisations were based on ambient measurement data. The split into
666 regimes is even more apparent on a linear flux scale. It must be noted that up
667 until now majority of global or regional scale models used one of the former four
668 parameterisations (Gong, 2003; Martensson et al., 2003; Clarke et al., 2006;
669 Fuentes et al., 2010) typically resulting in the overestimated mass concentrations
670 (e.g. (Textor et al., 2006; de Leeuw et al., 2011). Figure 7 reiterates the
671 conclusion made by Ovadnevaite et al. (2012) that the improvements were

672 needed in both whitecap parameterisation, now addressed by Callaghan (2013);
673 and the more realistic differential aerosol productivity term recently advanced by
674 Ovadnevaite et al.(2013). It is reasonable to suggest that the laboratory
675 experiments or the *in-situ* surf breaking waves were most likely unable to
676 realistically replicate air entrainment by the open ocean breaking waves and
677 consequently formed bubble plumes, resulting in unrealistic whitecap coverage
678 and/or size distributions. The most recently developed parameterisation by
679 Ovadnevaite et al. (2013) advanced even further by introducing Reynolds
680 number instead of a commonly used wind speed, thereby removing the
681 uncertainty related to the sea wave state (during rising or waning winds) and
682 implicitly containing sea surface water temperature and salinity which have been
683 both implicated to altering aerosol production (Martensson et al., 2003; Jaegle et
684 al., 2011; Zabori et al., 2012).

685 It can be argued that the new whitecap parameterisation of Callaghan et al.
686 (2013) coupled with Clarke et al. (2006), Fuentes et al. (2010) and Martensson et
687 al. (2003) parameterisations would bring all of them closer to the more recent
688 parameterisations, however, it is important to make few distinctive comments.
689 While the Gong-Monahan parameterisation has decreased the sea salt mass flux
690 when coupled with Callaghan (2013) whitecap parameterisation instead of the
691 original Monahan (Monahan et al., 1982) whitecap parameterisation, the size
692 resolved flux remains unrealistic due to the arbitrary adjusted submicron size
693 distribution below 0.2 μm (Gong, 2003). A single mode centred at around 100nm
694 fails to reproducing submicron size distributions observed in ambient air in
695 stormy maritime boundary layer (Ovadnevaite et al., 2013). Similarly, Clarke et
696 al. (2006), Fuentes et al. (2010) and Martensson et al. (2003) parameterisations,
697 even when coupled with Callaghan (2013) whitecap parameterisation, would still
698 predict concentrations far in excess of observed concentrations. The size resolved
699 fluxes are crucial in predicting direct and indirect climate effects and have to be
700 benchmarked against the ambient rather than the laboratory measurements unless
701 both reasonably agree.

702 The most significant limitation of the flux-gradient method is that it allowed
703 calculating fluxes up to moderate wind speed only. It is extremely rare that the
704 average wind speed above 15 m s^{-1} would be sustained over a week period.
705 Therefore, the sea spray source function method proposed by Ovadnevaite et al.

706 (2012; 2013) has to be considered as the more useful source function covering
707 wind speed range of up to 26 m s^{-1} . It should be also noted that the applicability
708 of the Clarke et al.(2006), Fuentes et al. (2010) and Martensson et al. (2003)
709 parameterisations come more questionably for higher wind speeds as the
710 divergence between the more recent parameterisations becomes progressively
711 greater and the slope of the dependency curve becomes unrealistically steep.

712

713 **3.4 WIOM and chlorophyll-a relationship**

714 Gantt et al. (2011) suggested that fractional contribution of organic matter in sea
715 spray particles depends not only on the biological activity in oceanic surface
716 waters, but also the wind speed at the point of emission. The data of this study
717 were examined according to the approach of Gantt et al. (2011). Figure 9
718 presents inter-relationship between fractional organic matter contribution to sea
719 spray ($OM_{ss}=WIOM/(WIOM+SS)$), wind speed using the data set of this study
720 which were not part of the dataset used by Gantt et al. (2011) and chlorophyll-a
721 concentration in the open ocean area upwind from Mace Head as examined
722 in Rinaldi et al. (2013). **Open ocean region was 10×10 deg or roughly 1000×1000**
723 **km upwind from Mace Head.** Only WIOM was taken into account in calculating
724 fractional contribution of OM in sea spray. Notwithstanding the fact that a
725 fraction of measured WSOM was associated with sea spray and formed by
726 processing primary WIOM, quantitative assessment is beyond current
727 knowledge. Both relationships were statistically significant ($P \ll 0.01$) and
728 explained 58% of the variance (top plots) suggesting an overlap. The obtained
729 relationships agree well with the relationship reported by Rinaldi et al. (2013)
730 based on an extended dataset (reaching 70% OM fractional contribution at $1.0 \mu\text{g}$
731 m^{-3}). Further, when the former relationship is coloured by the chlorophyll-a
732 concentration in the oceanic region upfront of the measurement location at Mace
733 Head, no apparent pattern can be discerned (bottom plot) apart from general
734 mutual relationship. It can be concluded, that while the OM_{ss} dependence on
735 wind speed is significant it may actually be weaker than the OM_{ss} and
736 chlorophyll-a relationship due to inter-dependence of wind speed and
737 chlorophyll-a – wind speed is higher in winter when chlorophyll-a concentration
738 is at its lowest and vice versa – thereby contributing to the excessive variance of
739 OM_{ss} and wind speed. Note that seasonal relationship between wind speed and

740 chlorophyll is simply a coincidence. For example, the effect of wind speed could
741 be elucidated if very low OM fractional contributions were often observed during
742 summer or high fractional contributions during winter which was never the case
743 with very few exceptions (only two). However, it is hardly a coincidence that the
744 two points (top right plot in Figure 9) with rather similar chlorophyll-*a*
745 concentration ($\sim 0.4 \mu\text{g m}^{-3}$) residing outside the 95% confidence bands are the
746 ones characterised with the lowest and the highest wind speed re-affirming that
747 the effect of wind speed is real, but difficult to separate from the OM_{ss} and
748 chlorophyll-*a* relationship. In conclusion, wind stress is the driver of primary sea
749 spray production, but biological productivity is modifying sea spray chemical
750 composition. Last but not least, it is important to note that the chlorophyll-*a*
751 concentration is only useful as a proxy of biological activity which can affect a
752 fraction of primary organic matter in sea spray in different ways depending on
753 the trophic level interactions.

754

755 **3.5 Seasonality of observed concentrations, gradients and fluxes**

756 The sampling strategy aimed at capturing two samples per month providing that
757 clean marine conditions were prevailing and each sample lasted on average 50%
758 of time during the calendar week. In reality, fifteen samples were collected
759 covering full year (April 2008 – May 2009) as listed in Table 1. The observed
760 seasonal cycle may not have been typical, but allowed to examine fluxes
761 associated with varying oceanic conditions throughout the calendar year.

762 The observed chemical species concentrations have been typical of those
763 documented at Mace Head by Yoon et al. (2007) and Ovadnevaite et al. (2014).
764 Sea salt concentrations and respective fluxes were generally the largest in winter
765 ($0.2\text{-}0.85 \mu\text{g m}^{-3}$ and $0.9\text{-}2.5 \text{ng m}^{-2} \text{s}^{-1}$, respectively) and the smallest in summer
766 ($0.07\text{-}0.5 \mu\text{g m}^{-3}$ and $0.1\text{-}0.6 \text{ng m}^{-2} \text{s}^{-1}$, respectively) which was mainly due to
767 the wind pattern over the North East Atlantic (Jennings et al., 2003; O'Dowd et
768 al., 2014). However, occurrence of deep low pressure system in e.g. September
769 2008 with corresponding high winds resulted in high sea salt concentrations and
770 large fluxes despite seasonal pattern suggesting otherwise. Therefore, sea salt
771 fluxes should be considered independent of the season and dependant on the
772 wind speed. On the other hand, it has been suggested that sea salt can be replaced
773 in primary sea spray by primary marine OM (Oppo et al., 1999; Facchini et al.,

774 2008b) in which case sea salt fluxes estimated from observed concentrations
775 would become smaller. This is at least partially reflected in the differences
776 between sea salt and sea spray fluxes and the larger respective sea spray flux
777 uncertainties. Also, the stronger sea salt and wind speed power law relationship
778 compared to pure sea salt relationship presented in Ovadnevaite et al. (2012)
779 suggests that the smaller sea salt fluxes during summer may be due to the
780 aforementioned replacement effect and may have constrained the relationship to
781 the higher power. Furthermore, Vaishya et al. (2012) showed that aerosol
782 scattering dependence on the wind is different between contrasting seasons
783 suggesting the effect of primary marine OM on sea spray production. **However,**
784 **considering the uncertainties of the flux-gradient method, a quantitative proof of**
785 **the aforementioned effect was not possible.**

786 The WIOM concentrations and fluxes revealed a much more complex pattern.
787 The absolute concentrations were lower in winter (0.06 - 0.19 $\mu\text{g m}^{-3}$) and higher
788 in summer (0.1 - 0.44 $\mu\text{g m}^{-3}$) following the pattern of oceanic biological activity
789 lately reaffirmed by Ovadnevaite et al. (2014). The seasonal variation of WIOM
790 gradients and fluxes, however, was different as the gradients depended on
791 biological activity in the flux footprint region (0.2-10 km from the coast) while
792 the fluxes depended both on the biological activity and wind speed dependent sea
793 spray production in the flux footprint area. The three distinct profiles of WIOM
794 gradients presented in Figure 3 clustered in characteristic periods. The removal
795 gradient prevailed in late spring and early summer when biological activity was
796 waning close to the coast. Yoon et al. (2007) demonstrated that biological
797 activity revealed by chlorophyll proxy has been typically starting at the coast
798 early in the season and then gradually moving off-shore and northward, thereby
799 affecting the WIOM gradients and corresponding fluxes. The production gradient
800 manifested itself during late summer and early spring, reaffirming conclusions
801 made by Yoon et al. (2007) about the presence of two or more phytoplankton
802 bloom peaks during the biologically active season. The mixed WIOM profile
803 prevailed during autumn when biological activity was waning over the North
804 East Atlantic, but at the same time shifting closer to the coast. The spatial
805 resolution of satellite chlorophyll data and the large errors associated with coastal
806 interfaces in particular (Darecki and Stramski, 2004; Gregg and Casey, 2007)
807 prevented exploring the relationship between coastal biological activity and

808 WIOM gradients, fluxes and its fractional contribution to sea spray. Previous
809 chapter demonstrated that open ocean biological activity revealed by the
810 chlorophyll proxy upwind from Mace Head correlated well with the WIOM
811 fractional contribution to sea spray validating the seasonal pattern of WIOM
812 gradients and fluxes. Therefore, despite WIOM fluxes were found dependent on
813 biological activity in the flux footprint area (0.2-10km) that did not invalidate a
814 relationship between WIOM and chlorophyll in the open ocean over the North
815 East Atlantic. Recently, Long et al. (2014) demonstrated a diurnal signal in
816 primary marine OM production suggesting that sunlight-mediated biogenic
817 surfactants may have a previously overlooked role. However, time resolution of
818 the gradient samples (weekly) and randomness of clean sector sampling during
819 day and night, prevented exploring the effect in this study. However, the results
820 of this study do not contradict the above study either as the primary marine OM
821 production would be enhanced in summer compared to other seasons following
822 radiation pattern.

823

824 **3.6 Boundary layer filling time**

825 The boundary layer filling time helps to understand a conceptual relationship
826 between the species concentration and its corresponding flux. The calculated sea
827 salt fluxes allowed an estimation of an important parameter called boundary
828 layer filling time τ according to the following equation:

$$829 \quad F_{eff} = \frac{C \times H_{MBL}}{\tau} \quad (4)$$

830 where F_{eff} is the effective flux; C is the concentration; H_{MBL} is the height of
831 marine boundary layer.

832

833 The boundary layer filling time for each sampling period was calculated using
834 the measured boundary layer height (day or night providing clean sector
835 condition were met), calculated sea salt flux (Figure 6) and the absolute sea salt
836 concentration at 30m level assumed as representative of the well mixed boundary
837 layer. The surface mixed layer (SML) height obtained from LIDAR
838 measurements varied in the range of 846-1102 meters among the eight periods
839 for which overlapping LIDAR measurements were available. An occasional
840 formation of nocturnal boundary layer was ignored here due to the nature and

841 resolution of the gradient samples. The corresponding filling time range was
842 calculated as 0.9-5.1 days with the median value of 1.8 days. Similar values of
843 the time constant to reach equilibrium concentration in the boundary layer taking
844 into consideration particle sizes were obtained by Hoppel et al. (2002) and the
845 value of 2 used by Ovadnevaite et al. (2012) in calculating the sea salt mass flux
846 based on sea salt concentration measurement. It is important to note, however,
847 that the filling time constant is a feature of a particular low pressure system
848 arriving at the point of observation in a connecting flow. Moreover, the flux-
849 gradient method is independent of the filling time and pretty insensitive to
850 precipitation which would mainly affect the absolute concentration value not
851 used in this study (concentration gradient was used instead). All other things
852 equal, the absolute concentration in the well mixed boundary layer would
853 continuously increase at a given flux eventually reaching steady state. Figure 10
854 helps to visualise various relationships between the four parameters: sea salt
855 concentration, sea salt flux, wind speed and boundary layer filling time. The
856 shortest filling time was obtained for the periods of the highest flux when the
857 absolute concentration was at its lowest. Clearly, the strongest winds could not
858 be sustained over the long periods of time to achieve a proportionally high
859 absolute mass concentration.

860 The longest boundary layer filling times should be attributed to the series of
861 well-defined low pressure systems without significant precipitation and the
862 calculated flux should be representative of the entire region of concentration
863 footprint which is many tens to few hundred kilometres upwind from Mace Head
864 (Ceburnis et al., 2008).

865

866 **4 Conclusions**

867 Marine aerosol sources, sinks and chemical fluxes were studied over the entire
868 year by the gradient method. The chemical fluxes of primary species, such as sea
869 salt, and more generally sea-spray were found to show strong power law
870 relationship with the wind speed. The power law exponent of sea salt mass
871 source function was 3.15 which was fractionally higher than the generally
872 considered cubic power law relationship. The flux versus wind speed relationship
873 of WIOM was found to be linear resulting from a dependence on the biological
874 activity in oceanic waters as supported by the linear dependence of fractional

875 contribution of organic matter on chlorophyll-a concentration and the power law
876 relationship of sea spray production. The study of certain secondary species
877 (nitrate, oxalate, MSA, WSON) was performed for the first time revealing their
878 mainly secondary origin, but also interactions with primary sea spray. The
879 seasonal pattern of concentrations, gradients and corresponding fluxes
880 highlighted complex interactions between biological activity, especially in the
881 flux footprint area, and wind driven sea spray production. The marine boundary
882 layer filling time was found to be variable in the range of 1 to 5 days linking
883 species concentration, flux and wind speed. The obtained sea salt mass flux and
884 wind speed parameterisation compared very well with other parameterisations
885 which used carefully selected ambient measurement data. The comparison with
886 the range of available flux-wind-speed parameterisations revealed significant
887 advances in the development of the sea spray source function for the benefit of
888 global climate models.

889

890 **Acknowledgements**

891 The work of this paper has been funded by the EPA Ireland STRIVE project
892 EASI-AQCIS and D. Ceburnis fellowship project Research Support for Mace
893 Head. The European Space Agency (Support To Science Element: Oceanflux
894 Sea Spray Aerosol) and EC ACTRIS Research Infrastructure Action under the
895 7th Framework Programme support are acknowledged as well. The authors
896 would like to thank A. Callaghan from Scripps Institution of Oceanography,
897 USA for sharing his data; Salvatore Marullo from Italian National Agency for
898 New Technologies, Energy and Sustainable Economic Development (ENEA),
899 Frascati, Italy and Rosalia Santoleri from Institute of Atmospheric Sciences and
900 Climate, National Research Council, Rome, Italy for providing satellite
901 chlorophyll data.

902

903 **References**

- 904 Ahlm, L., Nilsson, E. D., Krejci, R., Martensson, E. M., Vogt, M., and Artaxo,
905 P.: Aerosol number fluxes over the Amazon rain forest during the wet season,
906 *Atmos. Chem. Phys.*, 9, 9381-9400, 2009.
- 907 Blanchard, D. C.: Sea-to-air transport of surface active material, *Science*, 146,
908 396-397, 1964.
- 909 Brooks, I. M., Yelland, M. J., Upstill-Goddard, R. C., Nightingale, P. D., Archer,
910 S., d'Asaro, E., Beale, R., Beatty, C., Blomquist, B., Bloom, A. A., Brooks, B. J.,
911 Cluderay, J., Coles, D., Dacey, J., DeGrandpre, M., Dixon, J., Drennan, W. M.,
912 Gabriele, J., Goldson, L., Hardman-Mountford, N., Hill, M. K., Horn, M., Hsueh,
913 P. C., Huebert, B., de Leeuw, G., Leighton, T. G., Liddicoat, M., Lingard, J. J.
914 N., McNeil, C., McQuaid, J. B., Moat, B. I., Moore, G., Neill, C., Norris, S. J.,
915 O'Doherty, S., Pascal, R. W., Prytherch, J., Rebozo, M., Sahlee, E., Salter, M.,
916 Schuster, U., Skjelvan, I., Slagter, H., Smith, M. H., Smith, P. D., Srokosz, M.,
917 Stephens, J. A., Taylor, P. K., Telszewski, M., Walsh, R., Ward, B., Woolf, D.
918 K., Young, D., and Zemmelenk, H.: Physical Exchanges at the Air-Sea Interface
919 UK-Solas Field Measurements, *Bulletin of the American Meteorological Society*,
920 90, 629-644, 10.1175/2008bams2578.1, 2009.
- 921 Buzorius, G., Rannik, U., Makela, J. M., Vesala, T., and Kulmala, M.: Vertical
922 aerosol particle fluxes measured by eddy covariance technique using
923 condensational particle counter, *Journal of Aerosol Science*, 29, 157-171,
924 10.1016/s0021-8502(97)00458-8, 1998.
- 925 Callaghan, A., de Leeuw, G., Cohen, L., and O'Dowd, C. D.: Relationship of
926 oceanic whitecap coverage to wind speed and wind history, *Geophys. Res. Lett.*,
927 35, L23609,
928 10.1029/2008gl036165, 2008.
- 929 Callaghan, A. H.: An improved whitecap timescale for sea spray aerosol
930 production flux modeling using the discrete whitecap method, *J. Geophys. Res.-*
931 *Atmos.*, 118, 9997-10010, 10.1002/jgrd.50768, 2013.
- 932 Cavalli, F., Facchini, M. C., Decesari, S., Mircea, M., Emblico, L., Fuzzi, S.,
933 Ceburnis, D., Yoon, Y. J., O'Dowd, C. D., Putaud, J. P., and Dell'Acqua, A.:
934 Advances in characterization of size-resolved organic matter in marine aerosol
935 over the North Atlantic, *J. Geophys. Res.-Atmos.*, 109, D24215,
936 10.1029/2004jd005137, 2004.
- 937 Ceburnis, D., Garbaras, A., Szidat, S., Rinaldi, M., Fahrni, S., Perron, N.,
938 Wacker, L., Leinert, S., Remeikis, V., Facchini, M. C., Prevot, A. S. H.,
939 Jennings, S. G., Ramonet, M., and O'Dowd, C. D.: Quantification of the
940 carbonaceous matter origin in submicron marine aerosol by C-13 and C-14
941 isotope analysis, *Atmos. Chem. Phys.*, 11, 8593-8606, 10.5194/acp-11-8593-
942 2011, 2011.
- 943 Ceburnis, D., O'Dowd, C. D., Jennings, G. S., Facchini, M. C., Emblico, L.,
944 Decesari, S., Fuzzi, S., and Sakalys, J.: Marine aerosol chemistry gradients:

- 945 Elucidating primary and secondary processes and fluxes, *Geophys. Res. Lett.*, 35,
946 L07804, 10.1029/2008gl033462, 2008.
- 947 Charlson, R. J., Lovelock, J. E., Andreae, M. O., and Warren, S. G.: Oceanic
948 phytoplankton, atmospheric sulfur, cloud albedo and climate, *Nature*, 326, 655-
949 661, 1987.
- 950 Clarke, A. D., Owens, S. R., and Zhou, J. C.: An ultrafine sea-salt flux from
951 breaking waves: Implications for cloud condensation nuclei in the remote marine
952 atmosphere, *J. Geophys. Res.-Atmos.*, 111, 10.1029/2005jd006565, 2006.
- 953 Coe, H., Allan, J. D., Alfarra, M. R., Bower, K. N., Flynn, M. J., McFiggans, G.
954 B., Topping, D. O., Williams, P. I., O'Dowd, C. D., Dall'Osto, M., Beddows, D.
955 C. S., and Harrison, R. M.: Chemical and physical characteristics of aerosol
956 particles at a remote coastal location, Mace Head, Ireland, during NAMBLEX,
957 *Atmos. Chem. Phys.*, 6, 3289-3301, 2006.
- 958 Cooke, W. F., Jennings, S. G., and Spain, T. G.: Black carbon measurements at
959 Mace Head, 1989-1996, *J. Geophys. Res.-Atmos.*, 102, 25339-25346,
960 10.1029/97jd01430, 1997.
- 961 Dall'Osto, M., Ceburnis, D., Monahan, C., Worsnop, D. R., Bialek, J., Kulmala,
962 M., Kurten, T., Ehn, M., Wenger, J., Sodeau, J., Healy, R., and O'Dowd, C.:
963 Nitrogenated and aliphatic organic vapors as possible drivers for marine
964 secondary organic aerosol growth, *J. Geophys. Res.-Atmos.*, 117,
965 10.1029/2012jd017522, 2012.
- 966 Darecki, M., and Stramski, D.: An evaluation of MODIS and SeaWiFS bio-
967 optical algorithms in the Baltic Sea, *Remote Sensing of Environment*, 89, 326-
968 350, 10.1016/j.rse.2003.10.012, 2004.
- 969 de Leeuw, G., Andreas, E. L., Anguelova, M. D., Fairall, C. W., Lewis, E. R.,
970 O'Dowd, C., Schulz, M., and Schwartz, S. E.: Production flux of sea spray
971 aerosol, *Reviews of Geophysics*, 49, Rg2001, 10.1029/2010rg000349, 2011.
- 972 Decesari, S., Finessi, E., Rinaldi, M., Paglione, M., Fuzzi, S., Stephanou, E. G.,
973 Tzias, T., Spyros, A., Ceburnis, D., O'Dowd, C., Dall'Osto, M., Harrison, R.
974 M., Allan, J., Coe, H., and Facchini, M. C.: Primary and secondary marine
975 organic aerosols over the North Atlantic Ocean during the MAP experiment, *J.*
976 *Geophys. Res.-Atmos.*, 116, D22210, 10.1029/2011jd016204, 2011.
- 977 Decesari, S., Mircea, M., Cavalli, F., Fuzzi, S., Moretti, F., Tagliavini, E., and
978 Facchini, M. C.: Source attribution of water-soluble organic aerosol by nuclear
979 magnetic resonance spectroscopy, *Environ. Sci. Technol.*, 41, 2479-2484, Doi
980 10.1021/Es061711l, 2007.
- 981 Facchini, M. C., Decesari, S., Rinaldi, M., Carbone, C., Finessi, E., Mircea, M.,
982 Fuzzi, S., Moretti, F., Tagliavini, E., Ceburnis, D., and O'Dowd, C. D.: Important
983 Source of Marine Secondary Organic Aerosol from Biogenic Amines, *Environ.*
984 *Sci. Technol.*, 42, 9116-9121, 10.1021/Es8018385, 2008a.

- 985 Facchini, M. C., Rinaldi, M., Decesari, S., Carbone, C., Finessi, E., Mircea, M.,
986 Fuzzi, S., Ceburnis, D., Flanagan, R., Nilsson, E. D., de Leeuw, G., Martino, M.,
987 Woeltjen, J., and O'Dowd, C. D.: Primary submicron marine aerosol dominated
988 by insoluble organic colloids and aggregates, *Geophys. Res. Lett.*, 35, L17814,
989 10.1029/2008gl034210, 2008b.
- 990 Farmer, D. K., Kimmel, J. R., Phillips, G., Docherty, K. S., Worsnop, D. R.,
991 Sueper, D., Nemitz, E., and Jimenez, J. L.: Eddy covariance measurements with
992 high-resolution time-of-flight aerosol mass spectrometry: a new approach to
993 chemically resolved aerosol fluxes, *Atmospheric Measurement Techniques*, 4,
994 1275-1289, 10.5194/amt-4-1275-2011, 2011.
- 995 Fratini, G., Ciccioli, P., Febo, A., Forgiione, A., and Valentini, R.: Size-
996 segregated fluxes of mineral dust from a desert area of northern China by eddy
997 covariance, *Atmos. Chem. Phys.*, 7, 2839-2854, 2007.
- 998 Fuentes, E., Coe, H., Green, D., de Leeuw, G., and McFiggans, G.: On the
999 impacts of phytoplankton-derived organic matter on the properties of the primary
1000 marine aerosol - Part 1: Source fluxes, *Atmos. Chem. Phys.*, 10, 9295-9317, DOI
1001 10.5194/acp-10-9295-2010, 2010.
- 1002 Gaman, A., Rannik, U., Aalto, P., Pohja, T., Siivola, E., Kulmala, M., and
1003 Vesala, T.: Relaxed eddy accumulation system for size-resolved aerosol particle
1004 flux measurements, *Journal of Atmospheric and Oceanic Technology*, 21, 933-
1005 943, 10.1175/1520-0426, 2004.
- 1006 Gantt, B., Meskhidze, N., Facchini, M. C., Rinaldi, M., Ceburnis, D., and
1007 O'Dowd, C.: Wind speed dependent size-resolved parameterization for the
1008 organic mass fraction of sea spray aerosol, *Atmos. Chem. Phys.*, 11, 8777-8790,
1009 10.5194/acp-11-8777-2011, 2011.
- 1010 Geever, M., O'Dowd, C. D., van Ekeren, S., Flanagan, R., Nilsson, E. D., de
1011 Leeuw, G., and Rannik, U.: Submicron sea spray fluxes, *Geophys. Res. Lett.*, 32,
1012 Artn L15810, 10.1029/2005gl023081, 2005.
- 1013 Gong, S. L.: A parameterization of sea-salt aerosol source function for sub- and
1014 super-micron particles, *Glob. Biogeochem. Cycle*, 17, 10.1029/2003gb002079,
1015 2003.
- 1016 Gregg, W. W., and Casey, N. W.: Sampling biases in MODIS and SeaWiFS
1017 ocean chlorophyll data, *Remote Sensing of Environment*, 111, 25-35,
1018 10.1016/j.rse.2007.03.008, 2007.
- 1019 Haeffelin, M., Angelini, F., Morille, Y., Martucci, G., Frey, S., Gobbi, G. P.,
1020 Lolli, S., O'Dowd, C. D., Sauvage, L., Xueref-Remy, I., Wastine, B., and Feist,
1021 D. G.: Evaluation of Mixing-Height Retrievals from Automatic Profiling Lidars
1022 and Ceilometers in View of Future Integrated Networks in Europe, *Bound.-Layer
1023 Meteor.*, 143, 49-75, 10.1007/s10546-011-9643-z, 2012.
- 1024 Heard, D. E., Read, K. A., Methven, J., Al-Haider, S., Bloss, W. J., Johnson, G.
1025 P., Pilling, M. J., Seakins, P. W., Smith, S. C., Sommariva, R., Stanton, J. C.,

- 1026 Still, T. J., Ingham, T., Brooks, B., De Leeuw, G., Jackson, A. V., McQuaid, J.
1027 B., Morgan, R., Smith, M. H., Carpenter, L. J., Carslaw, N., Hamilton, J.,
1028 Hopkins, J. R., Lee, J. D., Lewis, A. C., Purvis, R. M., Wevill, D. J., Brough, N.,
1029 Green, T., Mills, G., Penkett, S. A., Plane, J. M. C., Saiz-Lopez, A., Worton, D.,
1030 Monks, P. S., Fleming, Z., Rickard, A. R., Alfarra, M. R., Allan, J. D., Bower,
1031 K., Coe, H., Cubison, M., Flynn, M., McFiggans, G., Gallagher, M., Norton, E.
1032 G., O'Dowd, C. D., Shillito, J., Topping, D., Vaughan, G., Williams, P., Bitter,
1033 M., Ball, S. M., Jones, R. L., Povey, I. M., O'Doherty, S., Simmonds, P. G.,
1034 Allen, A., Kinnersley, R. P., Beddows, D. C. S., Dall'Osto, M., Harrison, R. M.,
1035 Donovan, R. J., Heal, M. R., Jennings, S. G., Noone, C., and Spain, G.: The
1036 North Atlantic Marine Boundary Layer Experiment (NAMBLEX). Overview of
1037 the campaign held at Mace Head, Ireland, in summer 2002, *Atmos. Chem. Phys.*,
1038 6, 2241-2272, 2006.
- 1039 Held, A., Niessner, R., Bosveld, F., Wrzesinsky, T., and Klemm, O.: Evaluation
1040 and application of an electrical low pressure impactor in disjunct eddy
1041 covariance aerosol flux measurements, *Aerosol Science and Technology*, 41,
1042 510-519, 10.1080/02786820701227719, 2007.
- 1043 Hoffman, E. J., and Duce, R. A.: Organic-carbon in marine atmospheric
1044 particulate matter - concentration and particle-size distribution, *Geophys. Res.*
1045 *Let.*, 4, 449-452, 1977.
- 1046 Hopkins, R. J., Desyaterik, Y., Tivanski, A. V., Zaveri, R. A., Berkowitz, C. M.,
1047 Tylliszczak, T., Gilles, M. K., and Laskin, A.: Chemical speciation of sulfur in
1048 marine cloud droplets and particles: Analysis of individual particles from the
1049 marine boundary layer over the California current, *J. Geophys. Res.-Atmos.*, 113,
1050 10.1029/2007jd008954, 2008.
- 1051 Hoppel, W. A., Frick, G. M., and Fitzgerald, J. W.: Surface source function for
1052 sea-salt aerosol and aerosol dry deposition to the ocean surface, *J. Geophys.*
1053 *Res.-Atmos.*, 107, 4382, 10.1029/2001jd002014, 2002.
- 1054 Jaegle, L., Quinn, P. K., Bates, T. S., Alexander, B., and Lin, J. T.: Global
1055 distribution of sea salt aerosols: new constraints from in situ and remote sensing
1056 observations, *Atmos. Chem. Phys.*, 11, 3137-3157, 10.5194/acp-11-3137-2011,
1057 2011.
- 1058 Jennings, S. G., Kleefeld, C., O'Dowd, C. D., Junker, C., Spain, T. G., O'Brien,
1059 P., Roddy, A. F., and O'Connor, T. C.: Mace head atmospheric research station
1060 characterization of aerosol radiative parameters, *Boreal Environment Research*,
1061 8, 303-314, 2003.
- 1062 Kawamura, K., and Sakaguchi, F.: Molecular distributions of water soluble
1063 dicarboxylic acids in marine aerosols over the Pacific Ocean including tropics, *J.*
1064 *Geophys. Res.-Atmos.*, 104, 3501-3509, 1999.
- 1065 Keane-Brennan, J.: Air to sea gas exchange of CO₂ in the north-east Atlantic
1066 Ocean, PhD Thesis, 2011.

- 1067 Keene, W. C., Maring, H., Maben, J. R., Kieber, D. J., Pszenny, A. A. P., Dahl,
1068 E. E., Izaguirre, M. A., Davis, A. J., Long, M. S., Zhou, X. L., Smoydzin, L., and
1069 Sander, R.: Chemical and physical characteristics of nascent aerosols produced
1070 by bursting bubbles at a model air-sea interface, *J. Geophys. Res.-Atmos.*, 112,
1071 D21202
1072 10.1029/2007jd008464, 2007.
- 1073 Leck, C., and Bigg, E. K.: Source and evolution of the marine aerosol - A new
1074 perspective, *Geophys. Res. Lett.*, 32, L19803, 10.1029/2005gl023651, 2005.
- 1075 Long, M. S., Keene, W. C., Kieber, D. J., Frossard, A. A., Russell, L. M.,
1076 Maben, J. R., Kinsey, J. D., Quinn, P. K., and Bates, T. S.: Light-enhanced
1077 primary marine aerosol production from biologically productive seawater,
1078 *Geophys. Res. Lett.*, 41, 2014GL059436, 10.1002/2014GL059436, 2014.
- 1079 Martensson, E. M., Nilsson, E. D., Buzorius, G., and Johansson, C.: Eddy
1080 covariance measurements and parameterisation of traffic related particle
1081 emissions in an urban environment, *Atmos. Chem. Phys.*, 6, 769-785, 2006.
- 1082 Martensson, E. M., Nilsson, E. D., de Leeuw, G., Cohen, L. H., and Hansson, H.
1083 C.: Laboratory simulations and parameterization of the primary marine aerosol
1084 production, *J. Geophys. Res.-Atmos.*, 108, 4297,
1085 10.1029/2002jd002263, 2003.
- 1086 Martin, C. L., Longley, I. D., Dorsey, J. R., Thomas, R. M., Gallagher, M. W.,
1087 and Nemitz, E.: Ultrafine particle fluxes above four major European cities,
1088 *Atmos. Environ.*, 43, 4714-4721, 10.1016/j.atmosenv.2008.10.009, 2009.
- 1089 Meng, Z., and Seinfeld, J. H.: Time scales to achieve atmospheric gas-aerosol
1090 equilibrium for volatile species, *Atmos. Environ.*, 30, 2889-2900,
1091 [http://dx.doi.org/10.1016/1352-2310\(95\)00493-9](http://dx.doi.org/10.1016/1352-2310(95)00493-9), 1996.
- 1092 Middlebrook, A. M., Murphy, D. M., and Thomson, D. S.: Observations of
1093 organic material in individual marine particles at Cape Grim during the First
1094 Aerosol Characterization Experiment (ACE 1), *J. Geophys. Res.-Atmos.*, 103,
1095 16475-16483, 1998.
- 1096 Milroy, C., Martucci, G., Lolli, S., Loaec, S., Sauvage, L., Xueref-Remy, I.,
1097 Lavric, J. V., Ciais, P., Feist, D. G., Biavati, G., and O'Dowd, C. D.: An
1098 Assessment of Pseudo-Operational Ground-Based Light Detection and Ranging
1099 Sensors to Determine the Boundary-Layer Structure in the Coastal Atmosphere,
1100 *Adv. Meteorol.*, 10.1155/2012/929080, 2012.
- 1101 Mochida, M., Kitamori, Y., Kawamura, K., Nojiri, Y., and Suzuki, K.: Fatty
1102 acids in the marine atmosphere: Factors governing their concentrations and
1103 evaluation of organic films on sea-salt particles, *J. Geophys. Res.-Atmos.*, 107,
1104 4325, 10.1029/2001jd001278, 2002.
- 1105 Monahan, E. C., Davidson, K. L., and Spiel, D. E.: Whitecap Aerosol
1106 Productivity Deduced from Simulation Tank Measurements, *Journal of*
1107 *Geophysical Research-Oceans and Atmospheres*, 87, 8898-8904, 1982.

- 1108 Monahan, E. C., and Muircheartaigh, I. O.: Optimal Power-Law Description of
1109 Oceanic Whitecap Coverage Dependence on Wind-Speed, *J Phys Oceanogr*, 10,
1110 2094-2099, 1980.
- 1111 Muller, C., Iinuma, Y., Karstensen, J., van Pinxteren, D., Lehmann, S., Gnauk,
1112 T., and Herrmann, H.: Seasonal variation of aliphatic amines in marine sub-
1113 micrometer particles at the Cape Verde islands, *Atmos. Chem. Phys.*, 9, 9587-
1114 9597, 2009.
- 1115 Nemitz, E., Jimenez, J. L., Huffman, J. A., Ulbrich, I. M., Canagaratna, M. R.,
1116 Worsnop, D. R., and Guenther, A. B.: An eddy-covariance system for the
1117 measurement of surface/atmosphere exchange fluxes of submicron aerosol
1118 chemical species - First application above an urban area, *Aerosol Science and
1119 Technology*, 42, 636-657, 10.1080/02786820802227352, 2008.
- 1120 Nilsson, E. D., Rannik, U., Kulmala, M., Buzorius, G., and O'Dowd, C. D.:
1121 Effects of continental boundary layer evolution, convection, turbulence and
1122 entrainment, on aerosol formation, *Tellus Ser. B-Chem. Phys. Meteorol.*, 53,
1123 441-461, 2001.
- 1124 Norris, S. J., Brooks, I. M., de Leeuw, G., Smith, M. H., Moerman, M., and
1125 Lingard, J. J. N.: Eddy covariance measurements of sea spray particles over the
1126 Atlantic Ocean, *Atmos. Chem. Phys.*, 8, 555-563, 2008.
- 1127 Norton, E. G., Vaughan, G., Methven, J., Coe, H., Brooks, B., Gallagher, M., and
1128 Longley, I.: Boundary layer structure and decoupling from synoptic scale flow
1129 during NAMBLEX, *Atmos. Chem. Phys.*, 6, 433-445, 2006.
- 1130 O'Connor, T. C., Jennings, S. G., and O'Dowd, C. D.: Highlights of fifty years of
1131 atmospheric aerosol research at Mace Head, *Atmospheric Research*, 90, 338-355,
1132 10.1016/j.atmosres.2008.08.014, 2008.
- 1133 O'Dowd, C., Ceburnis, D., Ovadnevaite, J., Vaishya, A., Rinaldi, M., and
1134 Facchini, M. C.: Do anthropogenic, continental or coastal aerosol sources impact
1135 on a marine aerosol signature at Mace Head?, *Atmos. Chem. Phys.*, 14, 10687-
1136 10704, 10.5194/acp-14-10687-2014, 2014.
- 1137 O'Dowd, C. D., and De Leeuw, G.: Marine aerosol production: a review of the
1138 current knowledge, *Philosophical Transactions of the Royal Society a-
1139 Mathematical Physical and Engineering Sciences*, 365, 1753-1774,
1140 10.1098/rsta.2007.2043, 2007.
- 1141 O'Dowd, C. D., Facchini, M. C., Cavalli, F., Ceburnis, D., Mircea, M., Decesari,
1142 S., Fuzzi, S., Yoon, Y. J., and Putaud, J. P.: Biogenically driven organic
1143 contribution to marine aerosol, *Nature*, 431, 676-680, 10.1038/Nature02959,
1144 2004.
- 1145 O'Dowd, C. D., Langmann, B., Varghese, S., Scannell, C., Ceburnis, D., and
1146 Facchini, M. C.: A combined organic-inorganic sea-spray source function,
1147 *Geophys. Res. Lett.*, 35, L01801, 10.1029/2007gl030331, 2008.

- 1148 O'Dowd, C. D., Lowe, J. A., and Smith, M. H.: The effect of clouds on aerosol
1149 growth in the rural atmosphere, *Atmospheric Research*, 54, 201-221, 2000.
- 1150 O'Dowd, C. D., Smith, M. H., Consterdine, I. E., and Lowe, J. A.: Marine
1151 aerosol, sea-salt, and the marine sulphur cycle: A short review, *Atmos. Environ.*,
1152 31, 73-80, 1997.
- 1153 Oppo, C., Bellandi, S., Innocenti, N. D., Stortini, A. M., Loglio, G., Schiavuta,
1154 E., and Cini, R.: Surfactant components of marine organic matter as agents for
1155 biogeochemical fractionation and pollutant transport via marine aerosols, *Marine*
1156 *Chemistry*, 63, 235-253, 1999.
- 1157 Ovadnevaite, J., Ceburnis, D., Canagaratna, M., Berresheim, H., Bialek, J.,
1158 Martucci, G., Worsnop, D. R., and O'Dowd, C.: On the effect of wind speed on
1159 submicron sea salt mass concentrations and source fluxes, *J. Geophys. Res.-*
1160 *Atmos.*, 117, 10.1029/2011jd017379, 2012.
- 1161 Ovadnevaite, J., Ceburnis, D., Leinert, S., Dall'Osto, M., Canagaratna, M.,
1162 O'Doherty, S., Berresheim, H., and O'Dowd, C.: Submicron NE Atlantic marine
1163 aerosol chemical composition and abundance: Seasonal trends and air mass
1164 categorization, *J. Geophys. Res.-Atmos.*, 119, 11850-11863,
1165 10.1002/2013jd021330, 2014.
- 1166 Ovadnevaite, J., Manders, A., de Leeuw, G., Monahan, C., Ceburnis, D., and
1167 O'Dowd, C. D.: A sea spray aerosol flux parameterization encapsulating wave
1168 state, *Atmos. Chem. Phys. Discuss.*, 13, 23139-23171, 10.5194/acpd-13-23139-
1169 2013, 2013.
- 1170 Reible, D. D.: *Fundamentals of Environmental Engineering*, Taylor & Francis,
1171 544 pp., 1998.
- 1172 Rinaldi, M., Decesari, S., Carbone, C., Finessi, E., Fuzzi, S., Ceburnis, D.,
1173 O'Dowd, C. D., Sciare, J., Burrows, J. P., Vrekoussis, M., Ervens, B., Tsigaridis,
1174 K., and Facchini, M. C.: Evidence of a natural marine source of oxalic acid and a
1175 possible link to glyoxal, *J. Geophys. Res.-Atmos.*, 116, D16204,
1176 10.1029/2011jd015659, 2011.
- 1177 Rinaldi, M., Facchini, M. C., Decesari, S., Carbone, C., Finessi, E., Mircea, M.,
1178 Fuzzi, S., Ceburnis, D., Ehn, M., Kulmala, M., de Leeuw, G., and O'Dowd, C.
1179 D.: On the representativeness of coastal aerosol studies to open ocean studies:
1180 Mace Head - a case study, *Atmos. Chem. Phys.*, 9, 9635-9646, 2009.
- 1181 Rinaldi, M., Fuzzi, S., Decesari, S., Marullo, S., Santoleri, R., Provenzale, A.,
1182 von Hardenberg, J., Ceburnis, D., Vaishya, A., O'Dowd, C. D., and Facchini, M.
1183 C.: Is chlorophyll-a the best surrogate for organic matter enrichment in
1184 submicron primary marine aerosol?, *J. Geophys. Res.-Atmos.*, 118, 4964-4973,
1185 10.1002/jgrd.50417, 2013.
- 1186 Russell, L. M., Hawkins, L. N., Frossard, A. A., Quinn, P. K., and Bates, T. S.:
1187 Carbohydrate-like composition of submicron atmospheric particles and their
1188 production from ocean bubble bursting, *Proceedings of the National Academy of*

- 1189 Sciences of the United States of America, 107, 6652-6657,
1190 10.1073/pnas.0908905107, 2010.
- 1191 Sciare, J., Favez, O., Sarda-Esteve, R., Oikonomou, K., Cachier, H., and Kazan,
1192 V.: Long-term observations of carbonaceous aerosols in the Austral Ocean
1193 atmosphere: Evidence of a biogenic marine organic source, *J. Geophys. Res.-*
1194 *Atmos.*, 114, D15302, 10.1029/2009jd011998, 2009.
- 1195 Seinfeld, J. H., and Pandis, S. N.: Atmospheric chemistry and physics – from air
1196 pollution to climate change Wiley Interscience, New York, 1232 pp., 2006.
- 1197 Stull, R. B.: An Introduction to Boundary Layer Meteorology, Springer, Boston,
1198 680 pp., 1988.
- 1199 Textor, C., Schulz, M., Guibert, S., Kinne, S., Balkanski, Y., Bauer, S., Bernsten,
1200 T., Berglen, T., Boucher, O., Chin, M., Dentener, F., Diehl, T., Easter, R.,
1201 Feichter, H., Fillmore, D., Ghan, S., Ginoux, P., Gong, S., Kristjansson, J. E.,
1202 Krol, M., Lauer, A., Lamarque, J. F., Liu, X., Montanaro, V., Myhre, G., Penner,
1203 J., Pitari, G., Reddy, S., Seland, O., Stier, P., Takemura, T., and Tie, X.: Analysis
1204 and quantification of the diversities of aerosol life cycles within AeroCom,
1205 *Atmos. Chem. Phys.*, 6, 1777-1813, 2006.
- 1206 Turekian, V. C., Macko, S. A., and Keene, W. C.: Concentrations, isotopic
1207 compositions, and sources of size-resolved, particulate organic carbon and
1208 oxalate in near-surface marine air at Bermuda during spring, *J. Geophys. Res.-*
1209 *Atmos.*, 108, 4157, 10.1029/2002jd002053, 2003.
- 1210 Vaishya, A., Jennings, S. G., and O'Dowd, C.: Wind-driven influences on aerosol
1211 light scattering in north-east Atlantic air, *Geophys. Res. Lett.*, 39,
1212 10.1029/2011gl050556, 2012.
- 1213 Valiulis, D., Ceburnis, D., Sakalys, J., and Kvietkus, K.: Estimation of
1214 atmospheric trace metal emissions in Vilnius City, Lithuania, using vertical
1215 concentration gradient and road tunnel measurement data, *Atmos. Environ.*, 36,
1216 6001-6014, Pii S1352-2310(02)00764-1, 2002.
- 1217 Yoon, Y. J., Ceburnis, D., Cavalli, F., Jourdan, O., Putaud, J. P., Facchini, M. C.,
1218 Decesari, S., Fuzzi, S., Sellegri, K., Jennings, S. G., and O'Dowd, C. D.:
1219 Seasonal characteristics of the physicochemical properties of North Atlantic
1220 marine atmospheric aerosols, *J. Geophys. Res.-Atmos.*, 112, D04206,
1221 10.1029/2005jd007044, 2007.
- 1222 Zabori, J., Matisans, M., Krejci, R., Nilsson, E. D., and Strom, J.: Artificial
1223 primary marine aerosol production: a laboratory study with varying water
1224 temperature, salinity, and succinic acid concentration, *Atmos. Chem. Phys.*, 12,
1225 10709-10724, 10.5194/acp-12-10709-2012, 2012.
1226
1227

1228 Table 1. Gradient sample weekly collection time scale and the number of hours
 1229 each sample was sampled during 13 month period in 2008-2009.

Sampling period	Duration, h	Sampling period	Duration, h	Sampling period	Duration, h
10-15/04/2008	36.8	30/06-07/07/2008	24.4	11-18/12/2008	72.8
24-29/04/2008	72.6	14-22/07/2008	147.5	14-21/01/2009	74.8
29/04-07/05/2008	10.3	22-29/08/2008	146.5	25/02-04/03/2009	131.5
27/05-06/06/2008	53.0	08-18/09/2008	84.0	04-11/03/2009	121.5
25/06-30/06/2008	69.3	30/09-10/10/2008	106.7	05-12/05/2009	87.7

1230

1231

1232 Table 2. Absolute concentration ranges of measured chemical species.

Chemical species	Concentration range, $\mu\text{g m}^{-3}$
Sea salt (SS)	0.066-2.571
Nss SO ₄	0.042-0.829
NO ₃	0.001-0.037
NH ₄	0.001-0.127
MSA	0.002-0.428
WSOM	0.047-1.568
WIOM	0.061-0.990
WSON	0.001-0.071
DMA	0.001-0.052
DEA	0.001-0.082
Oxalate	0.002-0.059

1233

1234

1235

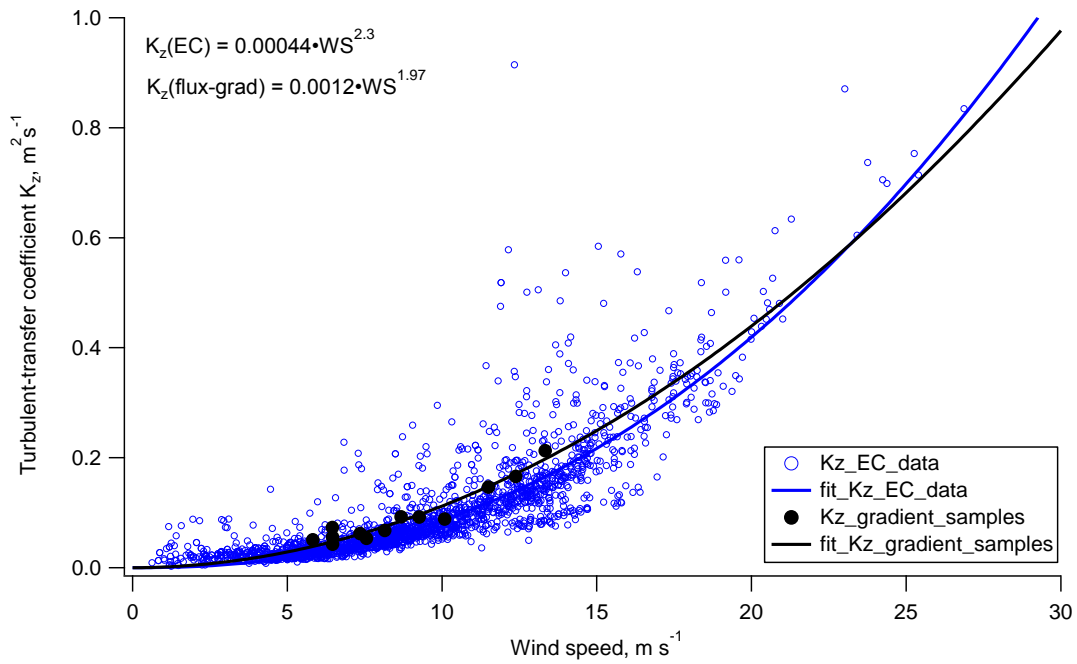
1236 Table 3. Uncertainty of the fitted parameters (\pm one standard deviation) of
1237 derived parameterisations in Figures 7-8.

Parameterisation	Linear coefficient	Power coefficient
Sea salt vs U_{10} $F_{SS}=0.0011U_{10}^{3.15}$	0.0011 ± 0.0014	3.15 ± 0.55
Sea spray vs U_{10} $F_{sea\ spray}=0.0007U_{10}^{3.4}$	0.0007 ± 0.001	3.4 ± 0.6
WIOM vs U_{10} $F_{WIOM}=-0.73+0.10U_{10}$	0.10 ± 0.03	Intercept -0.73 ± 0.28

1238

1239

1240



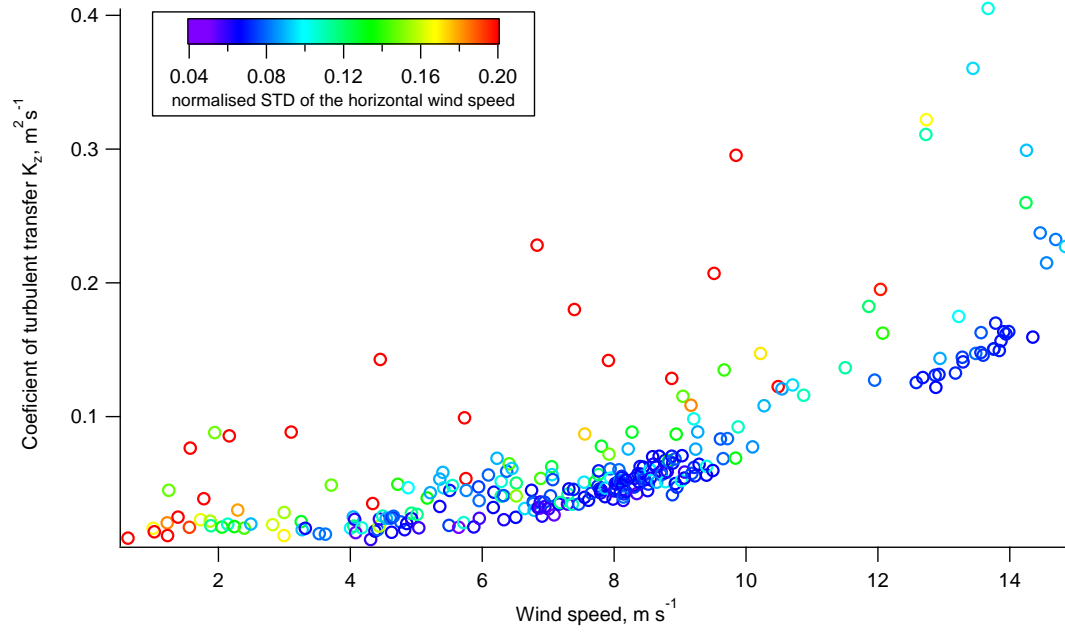
1241

1242

1243 Figure 1. A relationship between the coefficient of turbulent-transfer K_z (eddy
1244 diffusivity) and the horizontal wind speed in clean marine air over the whole
1245 sampling period. 30 min data from eddy covariance system (blue open circles)
1246 and averaged eddy covariance data for the duration of gradient samples (black
1247 circles) were both fitted by power law relationship.

1248

1249



1250

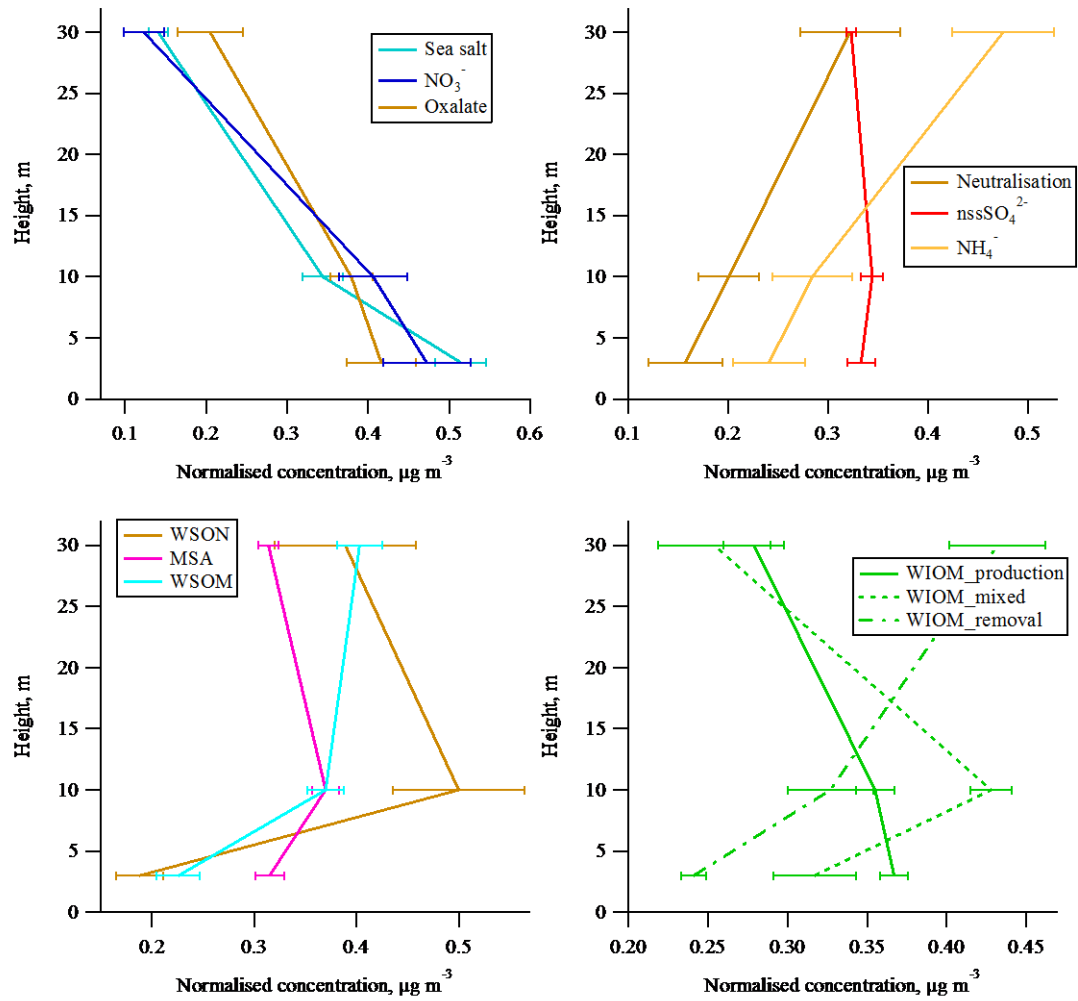
1251

1252 Figure 2. A dependence of the coefficient of turbulent-transfer K_z on the

1253 horizontal wind speed and normalised standard deviation of horizontal wind

1254 speed during April 2008 (a randomly chosen subset of data).

1255



1256

1257

1258 Figure 3. The gradient profiles of chemical species studied: species resembling

1259 primary production (top left); inorganic species resembling secondary production

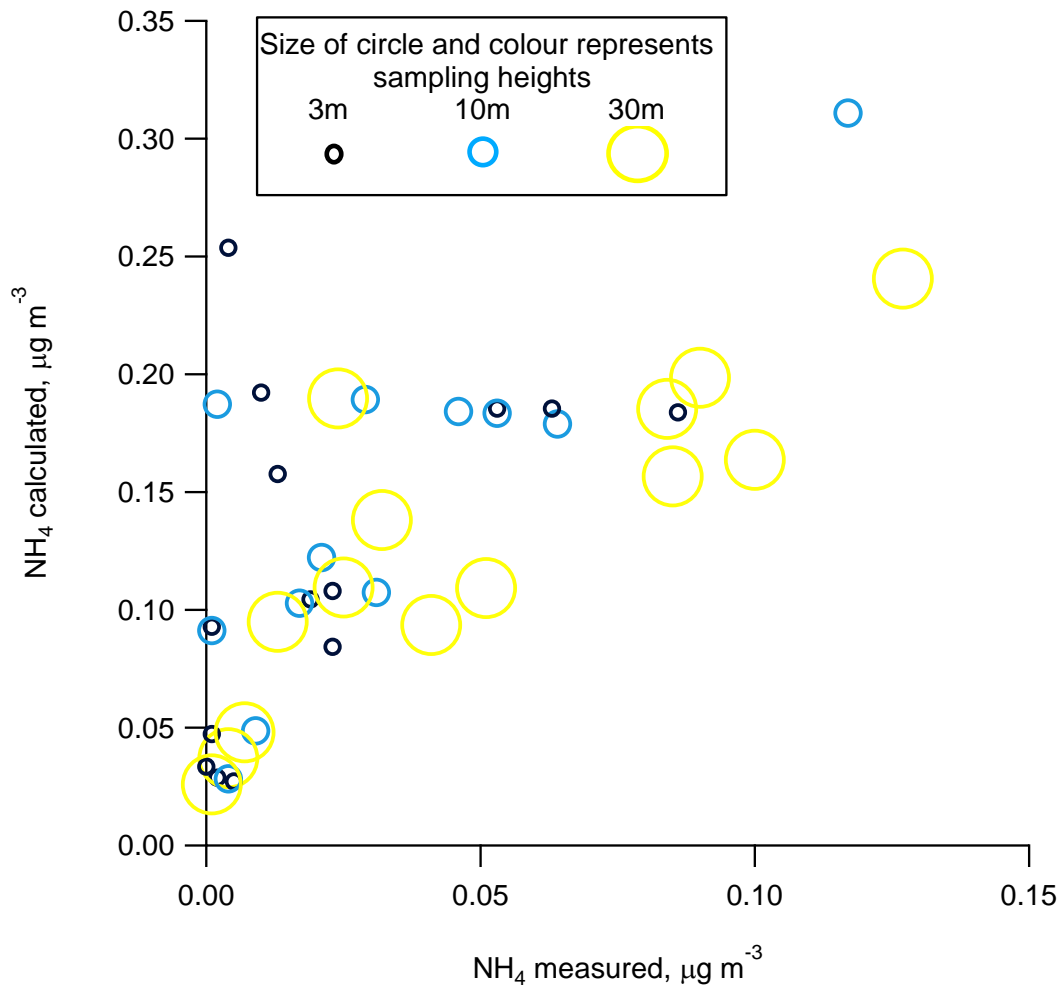
1260 (top right); organic secondary species (bottom left) and water insoluble organic

1261 matter split into production, removal and mixed profiles (bottom right).

1262

1263

1264



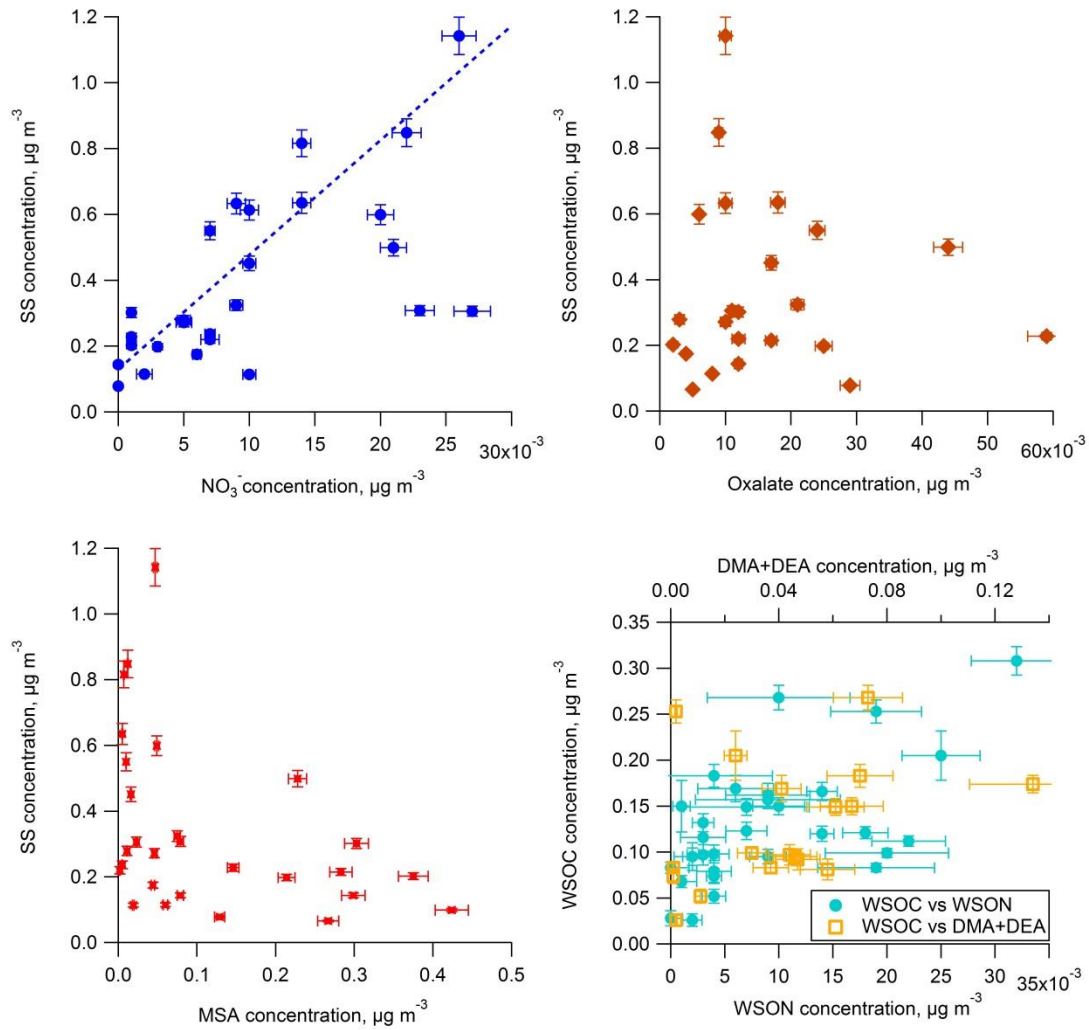
1265

1266

1267 Figure 4. A scatter plot of sulphate neutralisation by ammonium with respect to
1268 sampling height.

1269

1270

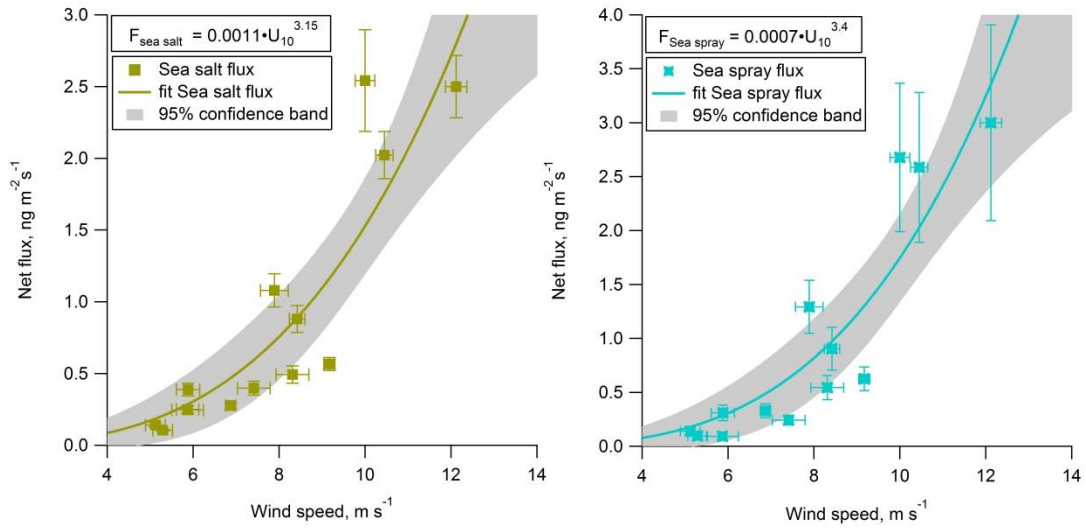


1271

1272

1273 Figure 5. Plots of sea salt and secondary species which resembled primary
 1274 production concentration pattern: SS vs NO_3^- (top left); SS vs Oxalate (top right);
 1275 SS vs MSA (bottom left) and WSOC vs WSON (also plotted as the sum of
 1276 dimethylamine and diethylamine)(bottom right). Note, that WSOC and WSON
 1277 concentration are presented as μg of carbon or nitrogen mass, respectively, while
 1278 all other species reported in absolute species concentrations.

1279



1280

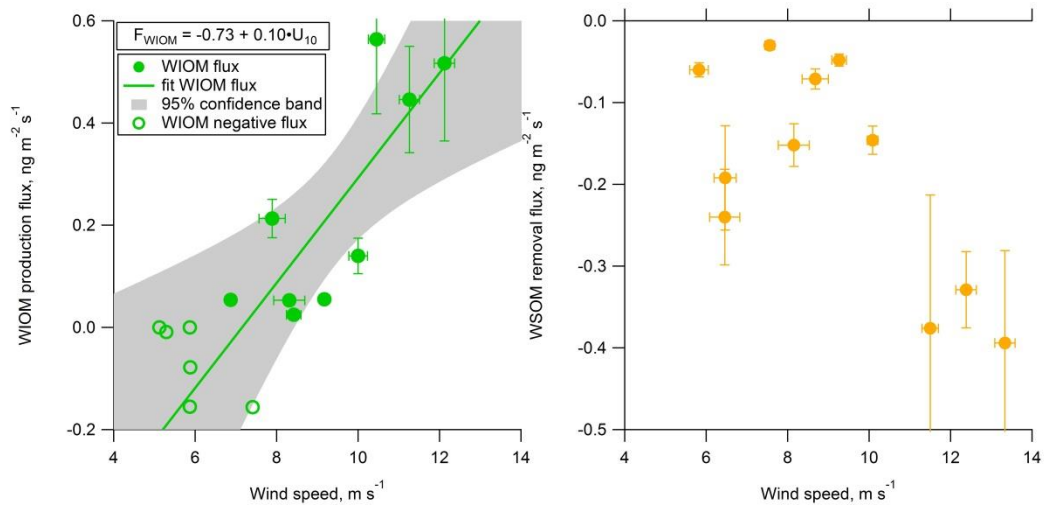
1281

1282 Figure 6. Sea salt and sea spray net production flux versus wind speed.

1283 Individual uncertainties of the flux and wind speed marked with caps while the

1284 grey area denotes 95% confidence bands of the fitted parameterisations.

1285



1286

1287

1288 Figure 7. Water insoluble organic matter net production flux versus wind speed

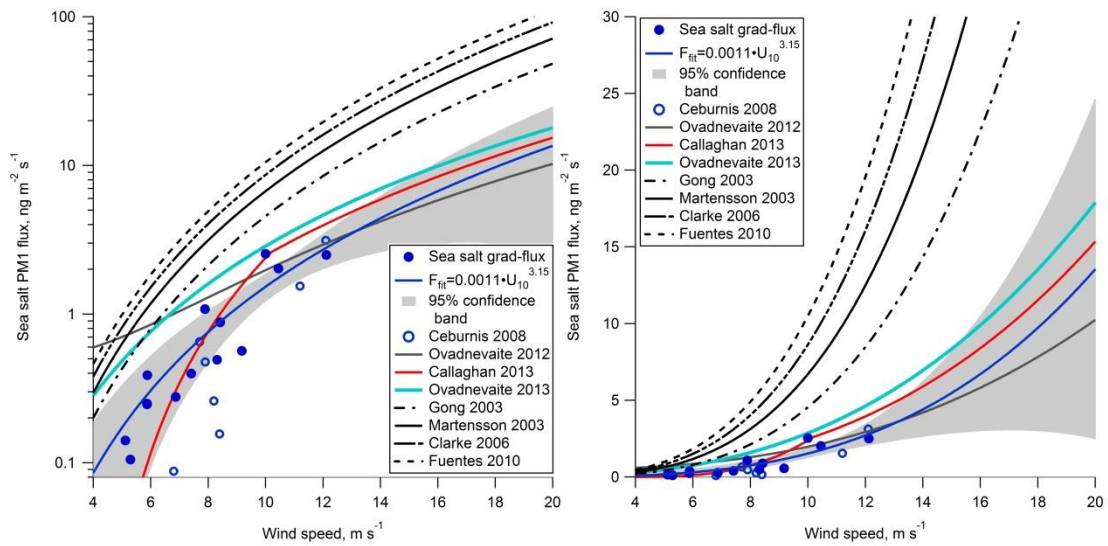
1289 (left) and the dependence of the WSOM removal rate on wind speed (right).

1290 Individual uncertainties of the flux and wind speed marked with caps while the

1291 grey area denotes 95% confidence bands of the fitted parameterisations. WSOM

1292 relationship was not parameterised due to large uncertainties.

1293



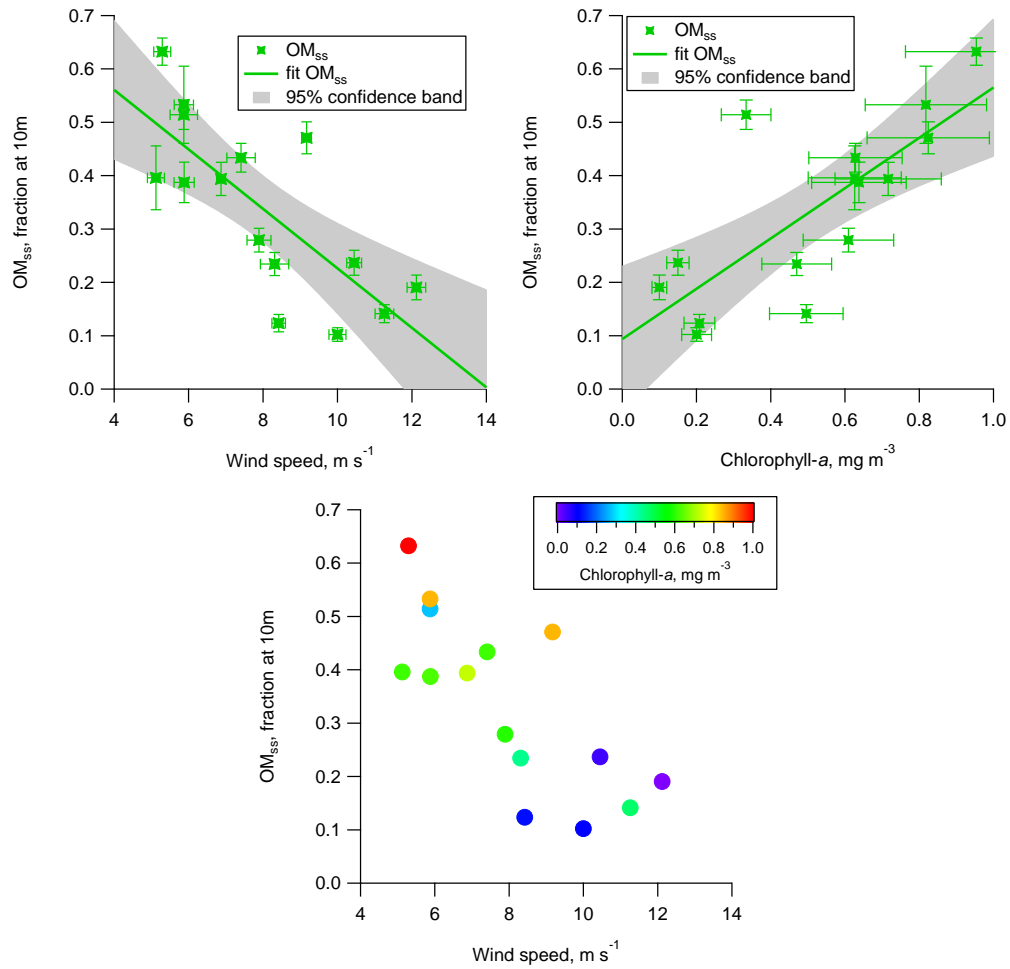
1294

1295

1296 Figure 8. A comparison of the most often used and recently developed sea spray
 1297 and wind speed parameterisations in log scale (left) and linear scale (right). The
 1298 grey area denotes the 95% confidence bands of the flux-gradient fitted
 1299 relationship.

1300

1301



1302

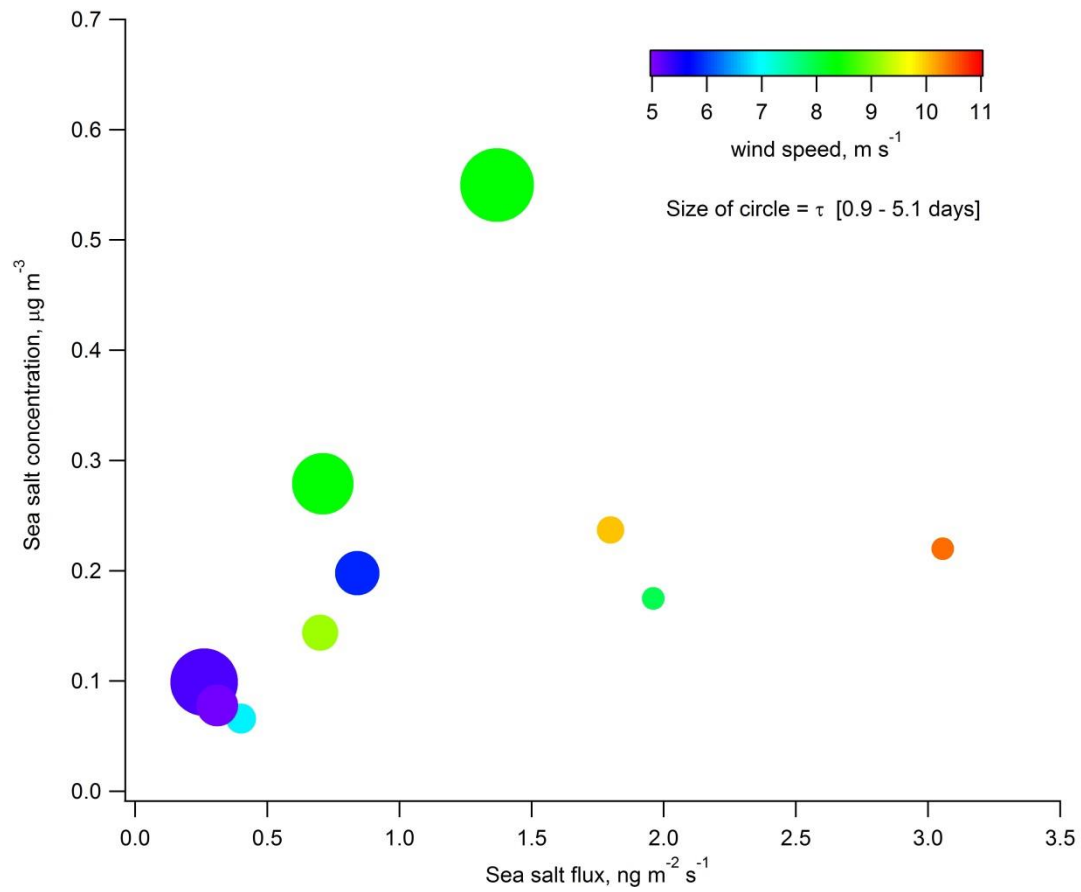
1303

1304 Figure 9. Effect of wind speed and chlorophyll-a concentration on the fractional
 1305 contribution of organic matter (OM_{ss}): OM_{ss} vs WS (top left); OM_{ss} vs
 1306 chlorophyll-a (top right) and OM_{ss} vs WS coloured by chlorophyll-a (bottom).

1307 Individual uncertainties of the flux and wind speed marked with caps while the
 1308 grey area denotes 95% confidence bands of the fitted parameterisation.

1309

1310



1311

1312

1313 Figure 10. A relationship between sea salt absolute concentration (y-axis), sea

1314 salt flux (x-axis), wind speed (colour) and boundary layer filling time (marker

1315 size).

1316

1317

1318
1319

Table S1. Measurement uncertainties of concentration profiles for individual chemical species.

ID sample	Height	NH4	NO3	WSON	WSOC	WIOC	Na	SO4	dma	dea	Oxa	MSA	Nss SO4
MH100408	3	6%	5%	92%	16%	11%	5%	5%	<DL	<DL	5%	5%	6%
MH100408	10	5%	5%	61%	13%	10%	5%	5%	<DL	<DL	5%	5%	6%
MH100408	30	5%	5%	55%	9%	9%	5%	5%	9%	15%	5%	5%	5%
MH240408	3	8%	5%	49%	10%	12%	5%	5%	<DL	<DL	5%	5%	6%
MH240408	10	5%	5%	27%	8%	10%	5%	5%	<DL	<DL	5%	5%	6%
MH240408	30	5%	29%	77%	6%	9%	5%	5%	9%	15%	5%	5%	5%
MH290408	3	29%	5%	<DL	49%	26%	5%	5%	<DL	<DL	<DL	5%	6%
MH290408	10	32%	5%	<DL	22%	29%	5%	5%	<DL	<DL	<DL	5%	6%
MH290408	30	13%	24%	10%	7%	15%	5%	5%	9%	15%	<DL	5%	5%
MH270508	3	5%	5%	<DL	8%	12%	5%	5%	<DL	<DL	5%	5%	6%
MH270508	10	5%	8%	41%	8%	10%	5%	5%	<DL	<DL	10%	5%	5%
MH270508	30	5%	<DL	125%	7%	10%	5%	5%	9%	15%	<DL	5%	5%
MH250608	3	20%	5%	34%	7%	15%	5%	5%	9%	<DL	5%	5%	7%
MH250608	10	5%	11%	77%	6%	11%	5%	5%	<DL	<DL	5%	5%	5%
MH250608	30	5%	<DL	<DL	5%	11%	5%	5%	9%	15%	<DL	5%	5%
MH300608	3	<DL	5%	<DL	22%	22%	5%	5%	<DL	<DL	5%	5%	6%
MH300608	10	<DL	5%	105%	19%	15%	5%	5%	<DL	<DL	5%	5%	6%
MH300608	30	7%	7%	15%	13%	13%	5%	5%	9%	15%	5%	5%	5%
MH140708	3	5%	32%	28%	6%	10%	5%	5%	9%	15%	5%	5%	5%
MH140708	10	5%	<DL	15%	5%	12%	5%	5%	<DL	<DL	5%	5%	5%
MH140708	30	5%	<DL	28%	5%	13%	5%	5%	9%	15%	5%	5%	5%
MH220808	3	5%	5%	23%	5%	19%	5%	5%	9%	15%	5%	5%	5%
MH220808	10	5%	5%	13%	5%	24%	5%	5%	<DL	<DL	5%	5%	5%
MH220808	30	5%	41%	63%	5%	21%	5%	5%	9%	15%	5%	5%	5%
MH080908	3	54%	5%	19%	11%	12%	5%	5%	<DL	15%	5%	5%	7%
MH080908	10	85%	5%	8%	7%	10%	5%	5%	<DL	<DL	5%	5%	6%
MH080908	30	5%	5%	18%	8%	12%	5%	5%	9%	15%	5%	5%	6%
MH011008	3	5%	8%	9780%	29%	14%	5%	5%	<DL	15%	<DL	5%	9%
MH011008	10	5%	5%	<DL	18%	11%	5%	5%	<DL	<DL	5%	5%	7%
MH011008	30	5%	10%	28%	15%	12%	5%	5%	9%	15%	22%	5%	7%
MH111208	3	17%	8%	<DL	38%	13%	5%	5%	<DL	<DL	7%	27%	9%
MH111208	10	<DL	5%	45%	15%	11%	5%	5%	<DL	<DL	6%	12%	7%
MH111208	30	5%	10%	<DL	14%	23%	5%	5%	9%	15%	8%	22%	6%
MH140109	3	23%	5%	<DL	23%	15%	5%	5%	<DL	<DL	10%	<DL	21%
MH140109	10	<DL	8%	<DL	13%	14%	5%	5%	9%	15%	11%	<DL	16%
MH140109	30	<DL	7%	52%	11%	25%	5%	5%	9%	15%	<DL	<DL	13%
MH250209	3	5%	5%	100%	10%	12%	5%	5%	<DL	<DL	5%	5%	7%
MH250209	10	5%	5%	12%	5%	14%	5%	5%	<DL	<DL	6%	5%	6%
MH250209	30	5%	5%	678%	8%	13%	5%	5%	9%	15%	5%	5%	6%
MH040309	3	5%	5%	<DL	<DL	5%	5%	5%	<DL	<DL	7%	5%	14%
MH040309	10	5%	5%	<DL	24%	13%	5%	5%	<DL	<DL	<DL	5%	12%
MH040309	30	6%	6%	40%	26%	17%	5%	5%	9%	15%	<DL	6%	7%
MH050509	3	5%	5%	33%	10%	11%	5%	5%	<DL	<DL	16%	5%	6%
MH050509	10	5%	5%	10%	6%	13%	5%	5%	<DL	<DL	9%	5%	6%
MH050509	30	5%	12%	23%	6%	19%	5%	5%	9%	15%	8%	5%	5%

1320
1321